AD-11549

RESTRICTED

RESTRICTED

15,125 | 15,125

Strut.1564 | Strut.1564

STRUCTURE SUB-COMMITTEE

AERONAUTICAL RESEARCH COUNCIL

An Experimental Study of a Transversely Stiffened Tapered Box Girder under Torsion and Bending.

- By -
Bruce Malcolm Falconer, B.E., Ph.D., D.I.C.

Communicated by Prof. A. J. Sutton Pippard

16th August, 19[illegible]

Summary

This paper describes an experimental investigation, carried out in the Civil Engineering Laboratories of the Imperial College of Science and Technology, of the strain distribution in a transversely stiffened tapered box of trapezoidal cross section under torsion and bending. The overall length of the box was 16 ft. 3 in. and the wall thicknesses were sufficient to prevent the plating from buckling under test loadings.

The distributions of direct and shear strains around representative cross sections are shown graphically. For comparison with existing theory, curves have been superimposed showing the strains according to the engineers' theory of bending, the Bredt-Batho theory of torsion, and the general theory of Argyris and Dunne. Two analyses have been made from the latter theory - one as an 'equivalent four boom tube' and the other as a tube with 'direct stress carrying covers'.

CONTENTS

RESTRICTED

1. Introduction

A number of theoretical papers have drawn attention to the limitations of the conventional engineers' theories of bending and torsion commonly used for finding the stress distribution in stressed skin tubular structures. These theories are strictly applicable only for long members of uniform cross section and do not apply in the regions of loads and restraints. Their simplicity, however, has encouraged their extension to structures where the premises are known to be invalid.

The more general theories, which have been presented to consider the effects of taper and the proximity of loads and restraints, must be judged both by their accuracy and their simplicity of application to particular structures. The present investigation has been designed to provide information for use in examining the basic premises of the new theories, and to assist in determining the range of usefulness of the conventional theories.

Prototype wing tests, as normally carried out, do not provide suitable data for this purpose as the stress distribution in actual wing structures is complicated both by buckling and by structural discontinuities, in addition to the characteristics which it is required to study. Furthermore the main purpose of full-scale wing tests is to establish the ultimate strength of the structures, and strain measurements have not been measured in sufficient detail for the present purpose.

1.1 The present investigation

The present investigation was proposed by the Structure Sub-Committee of the Aeronautical Research Council, who desired a detailed record of the strain distribution in a moderately tapered unswept box, which could be used, in particular, for an examination of the basic assumptions of the general theory of tubes published by Argyris and Dunne*. The maximum angle of taper of the box was limited to about ten degrees, owing to a restriction imposed by a premise of the general theory.

/

*The General Theory of Cylindrical and Conical Tubes under Torsion and Bending Loads, by J. Hadji-Argyris and P. C. Dunne, Journal of the Royal Aeronautical Society, 1947.

A special test specimen without structural discontinuities was designed for the test. In order that it should behave linearly with load, the skin thicknesses, though large in comparison with normal aircraft practice, were chosen so that buckling would not occur under test loadings. The structure has been tested under pure torsion and under combinations of bending and torsion. The results are presented graphically at the end of the report.

The work was carried out in the Civil Engineering Laboratories of the Imperial College of Science and Technology, London.

1.2 Existing theories

Although the problem of finding the stress distribution in tubular structures can be formulated in terms of the expressions of the classical theory of elasticity, a thorough theoretical analysis has not yet been made because of the very great difficulties encountered in mathematical development. It seems probable that numerical solutions could be obtained by successive applications of relaxation methods but unfortunately these would lack generality.

In existing theories the problem has been rendered tractable by assumptions which simplify the elastic properties of the construction material and prescribe the modes in which deformation may be considered.

It is a fundamental assumption of the conventional beam theory that the distributions of direct strains over cross sections are linear. With this assumption the basic problem is to determine the deflection of a line joining the centroidal axes of cross sections; one does not then have to consider the elastic deformation of the three-dimensional structure. In the Bredt-Batho theory of torsion, it is presumed that a purely torsional component of load at any cross section is dissipated as a constant shear traction which acts tangentially around the perimeter. With both these assumptions it has been found possible to calculate stress distributions from Hooke's Law and the equilibrium equations of statics.

It is reasonable to presume from the principle of Saint Venant that at regions remote from loads, restraints, and discontinuities, the stress distributions of the conventional theory approach the actual stress distributions. Unfortunately in aircraft structures the aspect ratio of components is often low and it is seldom possible to apply Saint Venant's Principle with any real justification. As the highest stresses usually occur in the region of loaded and restrained sections, the conventional or elementary theories are often not sufficiently accurate.

In recent years theories have appeared which allow a more general mode of deformation under load than is permitted by the conventional theories. Attempts have been made to compute skin stresses which satisfy the stress strain relationships of the theory of elasticity, but in general this requirement has been too stringent. However a great simplification can be introduced by assuming zero transverse direct stress and strain in the skin. As a result only one equation for the equilibrium of an element of the material need be considered. From such a premise, and by assuming an idealised geometrical form, Argyris and Dunne have evolved their general theory of tubes under torsion and bending loads.

2. Scope of the Investigation

The objects of the investigation have been to find the strain distribution in a moderately tapered, transversely stiffened, thin-walled duralumin box under torsion and bending, and to give a comparison with the strains calculated by the conventional engineers' theories and the general theory of Argyris and Dunne.

Plate 4/

Plate 1 and Fig.1 show the box which was built to fulfil, as closely as possible, the assumptions of the Argyris and Dunne theory. The box was symmetrical about its central transverse plane as in an aeroplane wing, to ensure complete axial constraint at the central cross section under symmetrical loadings, and to afford the possibility of check measurements in the second half of the structure.

The box was tested in bending, in pure torsion, and in bending plus torsion. The loads were applied successively at the tips and at the third points between the tip and root sections, and were reacted at the central cross section.

Distributions of direct and shear strains were measured around representative cross sections, with the use of electric resistance strain gauges fitted as in Fig.4. The measurements have been plotted in a standard form using the perimeter of cross section as a base, and theoretical strains have been superimposed in order to give a pictorial comparison of results. Two analyses have been made from the Argyris and Dunne theory - one as an 'equivalent four boom tube' and the other as a tube with 'direct stress carrying covers'.

The choice of a test box is discussed in Part 3, and a description of it is given in Part 4. The test frame and loading rig are described in Part 5, the experimental technique in Part 6, the strain measurements in Part 7, and the analytical treatment in Part 8. A brief non-mathematical review of the Argyris and Dunne theory is given in Appendix II.

3. Choice of a Test Box

It is common in the design of aircraft structures to assume that thin plating can only resist shear stresses. Portions of the plating which would otherwise have carried direct stresses may then be allotted to booms and stringers on the basis of an effective width theory. In cases where this premise is accepted the theory of Argyris and Dunne finds its simplest application. The computation is tolerably easy for tubes having from four to six booms, though it can become prohibitive when the booms are numerous.

Though such an application of the theory may be of greater practical importance than the more general treatment, and the departures from elementary theory due to shear lag and other effects can be much greater when longitudinal stiffening is present, it was considered undesirable to use such a box for the present project. For example, the present arbitrary allocation of plate areas to booms and stringers could lead to large errors if the plate were thick. However if the walls were sufficiently thin for their influence on the direct stress distribution to be apparently insignificant, they would surely buckle; this would cause the box to behave non-linearly and would complicate the experimental analysis unduly.

While from practical considerations of computation according to the Argyris and Dunne theory, it would have been convenient to test a four boomed tube with very thin walls, for the foregoing reason this was not done. Furthermore, the premise of the shear-stress-direct-stress allocation noted above, would introduce an assumption which is not fundamental to the general theory, but has merely been introduced for convenience in computing particular cases. Mathematically the assumption is equivalent to replacing a continuous function by a number of discrete steps and, unless the individual steps were small and sufficiently numerous, this could introduce appreciable error.

The/

The box used had transversely supported walls sufficiently thick not to buckle, and small corner angles; this was considered to be the best of the alternatives which could be conveniently constructed. The chosen taper was the greatest to which it was considered the theory could be reasonably applied for the purpose of the present investigation. The overall size was determined from considerations of taper, constructional limits, workmanship, size of available strain gauges, and the minimum convenient spacing of transverse diaphragms which would allow gauges to be fitted on the inside of the box after three sides had been assembled with the fourth left off for access. The thickness of the plating was chosen so that its critical buckling stresses would be appreciably higher than the working stresses, and any initial deflections of the plating would be very small fractions of the plate thickness.

4. Description of Test Box

The test structure was a box girder of trapezoidal cross section having a length of 16 ft. 3 in. and made of DTD.610 B duralumin. It was symmetrical about its central cross section and tapered linearly towards each tip so that the longitudinal generators of the surface met in common points beyond the ends of the box. The box is shown in Plate 1, and various details of the internal construction are shown in Plates 2 - 4.

At the centre of the structure a heavy, mild steel, box component having reinforced holes, was built inside the skin to permit access to strain gauges on the inner surface at the root. This steel structure had three parallel diaphragms, as shown in Plate 2. Because of its high rigidity, the cross sections which are alongside the outer diaphragms and contain the outer rows of rivets were regarded as axially constrained 'root cross sections' of the outboard portions of the box. Access to the inside was possible through holes in the covering between the inner and an outer diaphragm, and in the outer diaphragm.

At the tips and at the third-points between tip and root, mild steel diaphragms were fitted for dispersing the applied loads into the structure. These loading diaphragms may be seen in Plates 2 and 4, and eye-bolts which screwed into them through holes in the cover, are shown in Plates 1 and 4. The transverse shape of the box was maintained by duralumin diaphragms, spaced at uniform intervals along the length of the structure: these were parallel to the 'root cross sections' and also the central cross section.

The centre line of the rear spar was a straight line from tip to tip of the box, and the tip cross sections were half way between taper points and root cross sections. The principal dimensions of the structure are given below and in Fig.1.

Overall length	16 ft. 3 in.
Distance between root cross sections	15 in.
Distance from root to tip cross sections	90 in.
Spacing between loading diaphragms	30 in.
Spacing between stabilising diaphragms	6 in.
Distance between spars at root	30 in.
Depth of front spar at root	12 in.
Depth of rear spar at root	8 in.
Distance between spars at tip	15 in.
Thickness of covers	0.190 in.
Thickness of spars	0.157 in.
Thickness of webs of stabilizing diaphragms	0.080 in.
Thickness of webs of loading diaphragms	3/8 in.
Thickness of plating of central stiffening structure	½ in.

The spar web plates were flanged outwards at their edges and were joined to the covers by steel rivets (Plate 4). The length of leg of the 'corner angles', so formed, was kept as small as practicable. By suitably selecting rivet sizes and pitches the leg length was allowed to taper towards the tip in approximately the same manner as the rest of the box. The riveting at the corner angles can be seen in Plate 1.

In order that the diaphragms should offer the minimum of restraint to warping under load, the attachment angles of the stabilising diaphragms and the flanges of the loading diaphragms were slotted at intervals around their perimeters, as shown in Fig.2. To increase the rotational restraint of the diaphragms against buckling of the covers, the legs of the diaphragm attachment angles were propped from the web stiffeners as shown in Plate 3.

The central stiffening structure and the loading diaphragms were welded mild steel plates and the surfaces in contact with the skin were machined to a tolerance of 0.012 in. Light alloy castings would have been too costly and similar components of riveted construction would have been too cumbersome. It is probable that temperature stresses were introduced by the differing thermal coefficients of expansion of steel and duralumin but this was accepted as of little consequence, since the structure behaved linearly with load and cycles of strain readings were taken under practically constant temperatures.

The test loads were transmitted to the structure by high tensile steel eye-bolts, which were screwed into blocks of mild steel welded in line with the webs of the loading diaphragms, as shown in Plate 2. The applied loads were transferred from the blocks into the diaphragm webs and then dispersed around the perimeters. Only small distortion within the plane of cross section should have occurred at the loading diaphragms, as the shear rigidity of the steel webs was equivalent to that of duralumin one inch thick.

To/

To decrease the influence of the access holes upon the stress distribution nearby, stiffening straps were welded around the periphery of the holes on the inside of the central steel structure, and then joined to the central diaphragm so that the straps in effect bounded each adjacent pair of holes. In addition the central steel structure was made of half-inch plate and so was very stiff in comparison with the rest of the box. The half-inch steel plate and duralumin covering had a combined rigidity equivalent to duralumin [illegible] in. thick. These precautions ensured that the access holes had a negligible influence on the stress distributions at the root cross sections.

To limit the possibility of rivet slip at the root cross section, the covers and spars were made of continuous sheets from tip to tip of the box, and additional external cover plates were fitted over the region of the central stiffening structure. The front spar of the box was fitted last. Solid rivets were used for all connections except at the junctions of the diaphragms and the front spar where hollow Chobert rivets were used. The design and construction of the test box required the greatest care and thanks are due to the Fairey Aviation Company, who made the box, for maintaining a high standard of workmanship throughout.

5. <u>Loading Apparatus</u>

As a preliminary to the investigation, it was necessary to build a space frame for loading the box. Though the frame and loading apparatus have been made of a size and capacity convenient for the present test, they were designed for general use in structural testing and now remain as a part of the permanent Laboratory equipment. The test frame can be used for applying up to four tensile loads of [illegible] tons each, in vertical or transversely horizontal directions, anywhere within a space of 22 × 9½ × 9½ ft. In addition, one single tensile 50 ton load, or two orthogonal or two torsionally opposed tensile loads of up to 50 tons each, can be reacted in the central transverse plane of the structure.

As may be seen in Plate [illegible] the space frame consists of four parallel and vertical portal frames, which are set at right angles to their common longitudinal axis and then braced together. The bracing is carried externally on outriggers so that it will be clear of the loading apparatus. The laboratory floor is of timber on steel joists above a basement, and all live loadings had therefore to be equilibrated within the frame.

Loads are applied by hydraulic retracting jacks supported on beams spanning from an outer to an inner frame. The jacks can be moved along the beams, and the beams can be moved around the perimeter of the portal frames, as required. At ground level there is a control panel with an array of needle valves for operating the jacks, either individually or collectively. Measurements of load are made with statimeters and a proving ring; the latter is also used to recalibrate the statimeters at intervals during tests. It is estimated that the loads in the present investigation were measured within an error of 2%, or 50 lb whichever was the greater.

The test box was supported at its centre by four steel straps lying in the central transverse plane of the structure. So that the girder could be free to 'see saw' about its centre, the straps were pin jointed with universal links close to the girder. Under a very light push the tip could be moved up and down by 2 to 3 in.

The linkage for applying the test loadings is shown diagrammatically in Fig.2 and may be seen in detail in the various photographs. It was made mainly of high tensile steel and has the same load capacity as the test frame, for subsequent general use. The linkage was counterbalanced so that its dead weight was not applied to the test box, and so that the forces at the measuring instruments were either equal to the applied loads, or a fixed ratio of them, and did not require zero corrections.

The/

The box was loaded symmetrically, at a cross section on each side of the transverse centre plane, by forces statically equivalent to a vertical shear and a twisting moment in planes of application parallel to the root cross sections. The combined components of load were reacted at the centre by the four straps supporting the girder. As the straps could only resist tension four of them were necessary.

The applied loading is shown in the upper diagram of Fig.2 and the linkage chosen to obtain it in the lower diagram. If a symmetrical arrangement of jacks had been used, acting as in the upper diagram, then the shear component of load, F, would have had to be found from the difference in readings of the measuring instruments for the upward and downward loads. The percentage error in ΔF might then have been much higher than the error in F or $F + \Delta F$, particularly when ΔF was small.

Since the component of load ΔF produced the bending strains at the root, it was necessary to know its value within the same percentage error as the load F. This was possible with the linkage arrangement adopted as ΔF was measured directly. Further the orthogonal arrangement of forces ensured that the loads applied by the two horizontal jacks were equal, and, except for effects of elastic deformation of the box and test frame, were unaffected by slight vertical movements of the test structure. This was a great advantage, as the jacks operated at four separate pressures in order that the ratio of loads could be changed at the control panel. When adjusting the loads only three of the jacks needed to be operated. After a little practice each instrument could be adjusted for full load in about 15 sec.

6. <u>Measurement of strains</u>

Electric resistance strain gauges were attached around the root cross sections on both sides of the central stiffening structure and at five additional cross sections in one half of the box. Two of these were located on either side of the innermost loading diaphragm and the remaining three centrally in the three spaces between the loading diaphragm and the root cross section.

The location and distribution of gauges is shown in Fig.4. Standard single element gauges (Tinsley Type 6c, 100 ohm, 3/8 in. gauge length) were used, as rosette strain gauges were not available. They were attached in patterns of longitudinal and inclined gauges, to measure lineal strains along and at 45 degrees to the generators respectively. Gauges were placed, with the same orientation, on both the inner and outer surfaces of the plating, and the distributions were symmetrically disposed about the centres of the sides of cross section. Before attaching the gauges paper templates with rectangular holes cut in the desired patterns were glued on the inner and outer surfaces of the plating. The templates were located from 1/16 in. holes drilled through the plating at the ends of cross section sides, and the gauges were glued within the rectangles as may be seen in Plates 1 and 2.

Measurements of strain were made with a Baldwin-Southwark, SR4, 48 channel scanner recorder, recording graphically on circular charts. Over a thousand strain gauges were used, arranged in groups of forty. Each group was wired to a plug of an improvised forty point mercury switch, the base of which was connected permanently to forty channels of the recorder. By interchanging the plugs which fitted in the base, particular groups of gauges were quickly and easily selected for recording. The loading cycles had to be repeated for each plug until all desired measurements were recorded. The arrangement is shown in Photo 2.

It/

It was intended to reduce the labour of 'zero balancing' the gauge resistances prior to measurement, by using gauges with only a small tolerance of ± 0.2 ohms on their nominal resistance of 100 ohms, and also by using only specially selected gauges of 100.0 ohms as dummies. Unfortunately, after all gauges were fixed and the wiring was completed the resistance tolerance was found to be about ± 0.6 ohms which was too large for the measuring instrument.

An attempt was then made, by soldering short lengths of resistance wire in series with each gauge, to adjust all gauges plus their pairs of wires to within ± 0.05 ohms of a nominal resistance of 101 ohms. Had this been successful the labour of obtaining readings would have been approximately halved, since zero balancing would not have been necessary, as all readings would have been within the scale of the recorder charts. It was not fully achieved, but a great improvement was made and most gauges were finally within ± 0.2 ohm and at least half were within 0.1 ohm.

A calibration beam was used to check the reading of the recorder and the behaviour of sample gauges. No allowance was made for lateral sensitivity of the gauges, believed to be about 2% of the lateral strain. The strains were measured within an estimated error of $\pm 5 \times 10^{-5}$.

As a visual aid in reading the strains which had been recorded graphically on the circular charts of the Baldwin instrument, a turntable device was made having a scale of strain mounted on a quadrant arm. This may be seen slightly right of centre in Plate 9. The quadrant pivoted about the same relative point as the pen arm of the recorder. By rotating it until the zero of its scale coincided with the 'baseline' reading made at zero load, the scale could be read directly, without the inconvenience of mentally subtracting slight errors of the zero setting.

The test results were first plotted on graphs as shown in Figs. 5-7, which for convenience had been printed for each cross section with the grid lines and gauge orientations shown on the paper. Curves were drawn through the test results for similarly orientated gauges, mean values being taken for inner and outer gauges. The results were then replotted on graphs showing the full cross section. Axial direct strains were plotted directly; shear strains were plotted from the vertical intercepts between the curves for inclined gauges.

7. Experimental Strains

The test structure was loaded with concentrated forces applied at the tips and at the third points between tip and root sections. The forces were symmetrically disposed about the central cross section of the box and lay in planes parallel to the root cross section. They were transmitted to the box through the eye-bolts indicated in Fig.1 and shown in Photo 1. Conditions of loading ranged from vertical shears which mainly produced bending, through combined shear and torsion, to pure torsion.

Strains were measured at sections F to F of Fig.1. The results are shown graphically in Figs. 8 to 51. For convenience these have been shown in a standard form, using the perimeter of cross sections as a base. The loadings, measurement sections, and corresponding figure numbers of results are given in Table 1.

Table 1.

Table 1

Loadings at cross section 2/3 of distance from tip to root

Load	Where applied	Measured at Section	Shown in figure
20,000 lb	front eye-bolt	E, A, B, C, D	8, 10, 12, 14, 16
15,000 lb	" "		
20,000 lb	rear eye-bolt	E, A, B, C, D	9, 11, 13, 15, 17
15,000 lb	" "		
8,125 lb	one chord out from rear spar	A, B, C, D	37, 39, 41, 42
400,000 lb in.	(pure torque)	A, C, D	36, 40, 42

Loading at cross section 1/3 of distance from tip to root

Load	Where applied	Measured at Section	Shown in figure
10,000 lb	front eye-bolt	E, A, B, C, D, F	18, 20, 22, 24, 26, 28
10,000 lb	rear eye-bolt	E, A, B, C, D, F	19, 21, 23, 25, 27, 29
7,000 lb	One chord out from rear spar	A, B, C	45, 47, 49
300,000 lb in.	(pure torque)	A, B, C	44, 46, 48

Loading at tip cross section

Load	Where applied	Measured at Section	Shown in figure
6666 lb	front eye-bolt	A, B, (C, E, F)	30, 32, (34)
6666 lb	rear eye-bolt	A, B, (C, E, F)	31, 33, (35)

The experimental results for the box loaded principally in shear, that is by a single vertical force applied directly to an eye-bolt on each side of the central cross section, were obtained before the linkage for torsional loadings had been constructed. It can be seen from these that measurements made at sections E and A under the same loading conditions agreed very closely. The agreement as shown by comparison of Figs. 8 and 10, of 9 and 11, of 18 and 20, and of 19 and 21, was such that time was not wasted in later tests in taking readings on both sides of the central cross section of the box.

As/

As an aid in comparing results, the bending loads of 6666, 10,000 and 20,000 lb which were applied at the respective loading sections, had been chosen to produce the same bending moment, of 600,000 lb in. at the root cross section. The maximum stress corresponding to this moment was 8400 p.s.i. (according to elementary theory) and was appreciably less than the critical compressive stress of the cover plating due to the bending of the box (at least 9000 p.s.i. calculated on the assumption that the diaphragms gave only simple support to the covers).

It may be of interest to note that, though the construction was very good and maximum initial deflections of the plating only about 3% of its thickness, a number of the strain gauge results indicated that slight buckling occurred in some places at well below the critical stress. The 'buckling' was noticed most of all at section B when the 6666 lb loads were applied at the tip. Dial deflection gauges showed it to be 40×10^{-4} in. between diaphragms, or 2% of plate thickness, and to have increased approximately linearly with load.

Apart from the slight discrepancy in surface strains, the box behaved linearly with load. To help confirm this the results shown in Fig.51 were predicted by superimposing components found by taking the required fractions of Figs. 10 and 11 in order that the combined loadings would be statically equivalent to the loading of Fig.51. The prediction, shown in Fig.50, is reasonably close.

On completion of the tests it was found that of the 1056 electric resistance strain gauges fitted to the base only 21 were defective because of open circuits or large apparent zero drifting. Most of the defective gauges were on the inside of the box and had been damaged initially during assembly of the fourth side. It is perhaps remarkable that of the 1035 remaining serviceable gauges, measurements from only one have been ignored in plotting the results. This gauge was located inside the box on a cover at Section B, and consistently gave high readings under load, even though zero readings were repeatable. The readings from the corresponding gauge on the outer surface agreed with the trend of results from adjacent gauges on both sides of the plating.

8. Computed Strains

Strains have been computed both by conventional elementary theories and by the general theory of Argyris and Dunne. They have been plotted on the same graphs as the experimental results, to give a pictorial comparison between theory and experiment. The method of plotting will be understood by reference to the figures.

No attempt has been made to obtain 'experimental' stresses from measured strains, as it is considered more fundamental and simpler to compare measurements and computations directly. It may, however, be of interest to note that a strain of 4×10^{-4} in duralumin is equivalent to a unidirectional stress of 4000 p.s.i. (1.78 tons per sq.in.) or a shear stress of 1560 p.s.i. (0.696 tons per sq.in.).

A brief record of the computations is given in Appendix II. Two analyses have been made using the general theory of Argyris and Dunne - one treating the box as an 'equivalent four boom tube', and the other as a 'tube with direct stress carrying covers'.

Strains derived from the former analysis are shown on all diagrams of results. Where the correction stresses are too small to plot, or the curves may be confusing, the results have been tabulated alongside each graph. Strains from the latter analysis have been shown only against the results for torsion, and such other results where they appear to be significant. They are given fully in Table [illegible] for all loadings close to the root cross section.

9✓

9. Discussion of Results

9.1 General

As cross sections of the box have a horizontal axis of symmetry, the distributions of theoretical strain in the upper and lower halves are symmetrical in magnitude. Because of the sign convention adopted in plotting, the shear strains are of like sign and the direct strains of opposite sign. Inspection of the graphs shows close agreement between the experimental results for top and bottom covers and for the upper and lower halves of the spar webs. This confirms that the straining was linear with load.

An exception to this symmetrical behaviour is shown by the direct strain in the front spar web at Section C for loadings of Figs. 14 and 40. The deviation, which was checked by repeating the measurements, is not considered to be due to misbehaviour of the electric strain gauges on the web at that section, as the results shown in Figs. 24 and 25 are satisfactory. It may be caused by rivet slip or deformation in the neighbourhood of the loaded section, since the front spar was fitted last and hollow Chobert rivets had to be used to attach it to the internal diaphragms. Such behaviour does not occur at Section A, where it was possible to use solid rivets on all four sides of the root cross section, because of the proximity of the access holes.

In general the experimental results lie along continuous curves and relatively small individual scatter is apparent, and it may be inferred that the results are a faithful record of the straining of the box.

A general trend of the experimental results for 'shear' loadings shown in Figs. 8-31 is that the magnitudes of shear strain in the covers are given by lines of reverse curvature, whereas lines of single curvature are predicted by the elementary theories. The minimum slope of the experimental lines occurs at about the centre of the covers, where it is about half that of the elementary theories. The slope tends to remain constant over a central band about half the width of the covers, and then to increase towards the corners of the sections. This is particularly evident for loadings close to the root. As may also be seen from the graphs, the effect of altering the torsional component of the 'shear' loading is to displace the curve of shear strain from the base line by constant increments.

It may appear from Figs. 9 and 10, that the lines of experimental shear strain shown in the front spar are more sharply curved than is consistent with the large rate of change of direct strains with depth of the spar web.

Large appreciable deviation from linearity of direct strain over cross sections of the covers is evident for loading close to the root. At sections P and A of Figs. 5-11 a large decrease in direct strain was recorded near the centre of the covers, whilst at section C and D of Figs. 14 to 17 there was a large increase. When the other two sections were loaded deviations from linearity were very greatly reduced.

The experimental shear strains for pure torsion tend to remain constant in each wall of the box. This is particularly evident in the results for sections B and E of Figs. 44 and 45, where the distribution of strain is very simple. Greater deviations from uniformity of shear strain have been found for torsional loadings applied nearer the root.

Tho/

The 'torsion bending' direct strains, which have developed for the pure torque loadings, appear to be self equilibrating. They are of anticipated sign and are larger for the loading nearer the root.

The results for shear plus torque show characteristics of each loading.

9.2 Elementary theories

Figs. 22, 47 and 46 have been obtained for Section B when loadings of 'shear', torque plus shear, and pure torque respectively were applied at $r = 120''$. Section B was reasonably remote from loads and restraints, and examination of the results shows that the elementary theory has very good accuracy for each of the three loadings. Because of the statical equivalence of theoretical and true stresses, it can be seen that the shears, moments, and torques corresponding to the experimentally measured strains must have been in equilibrium with the applied loads. Hence the experimental technique was satisfactory, and the values of direct and shear moduli of elasticity found initially from tests of specimens of the material, and which were used in computation, remained representative of the fabricated structure.

A detailed comparison of theory and experiment may be made by studying the figures.

It is interesting to note where the maximum experimental shear strains differ appreciably from the maximum strains of the elementary theories. In Table 2 the differences, expressed as a percentage of the theoretical values, have been listed where these exceed 5 per cent. As the direct strains due to torque have no elementary theoretical values they have been listed, instead, as percentages of the single theory shear strains. In Fig. 36 the experimental shear strain is intermediate between the elementary and general theoretical values, whilst in Figs. 40 and 41 the general and experimental values are in close agreement. This is of importance as the greatest deviations, [illegible]% for pure torsion and 21% for torsion plus bending, have been found immediately inboard of the loading section at $r = 15[illegible]''$.

Table 2/

Table 2

Figure No.	Percentage deviation of maximum experimental strains from maximum strains of the elementary theories		
	Shear	Direct	Direct (due to pure torque)
8	+ 7	+ 20	
9		+ 9	
10	+13	+ 20	
11		+ 12	
12		- 6	
14		+ 50	
15	+ 8	+ 6	
20	+ 9	+ 9	
22	- 5		
36	+41		+38
37		+ 75	
39	+ 8		
40	+34		+25
41	+31	+350	+20
44	+10		+40
45	+ 6		
46			+19
47	+ 6		
48			+13
49		+ 15	

After the main tests were completed two inclined gauges, which may be seen at the upper left hand corner of Photo 9, where fixed on the outer surface of the rear spar web immediately inboard of the loading section at r = 120", as large deviations can be expected immediately inboard of inner loading sections. The readings from these two gauges indicated deviations of about +30% in shear strain for the torsional loading.

9.3 Theory of Argyris and Dunne

The computation for an 'equivalent four boom tube' was intended to give a first approximation to components of the self-equilibrating stresses due to torsional components of load. In this treatment the distribution of direct stress in each wall is presumed to be linear and shear lag and related effects are ignored. The computation for a tube with 'direct stress carrying covers', however, has been intended to give the self-equilibrating stresses for both torsional and shear components of load.

From/

From the results it can be seen that both treatments have given a fair estimate of the stresses due to torsional loadings, but the second treatment has not interpreted the 'lagging' of measured strains under shear loadings, as may be seen from Table [illegible]. Analytical results from the second treatment have not been plotted on the graphs for shear loadings, except for the webs of Figs. 8 and 9. For the loadings at $r = 150''$ the theoretical results of the second treatment have been listed in Table 6.

The results for pure torsion at $r = 150''$ are of interest as they show strain distributions close to the root and on each side of the loading section. At the root the torsion bending strains are in close agreement with the theory, though the shear strains are smaller than predicted, and are intermediate between those of the general and elementary theories. On each side of the loading section the shear strains of experiment and the general theory are in very good agreement, as may be seen in Figs. 40 and 42. This is of great importance as the recorded shear strain in the rear spar web immediately inboard of the loading section (see Fig.40) is about 3[illegible]% greater than is predicted by the Bredt-Batho theory.

The results for loadings combining torsion and shear exhibit characteristics of both the shear and torsion solutions.

The lateral straining of the plating was very small, and is consistent with the assumption that it is sufficiently small to be ignored. The lateral strain at the measurement sections could be obtained quite simply from the graphs of lineal strains, such as shown in Figs. 5 to 7, by subtracting the axial direct strain from the sum of the two inclined lineal strains which had been measured in orthogonal directions. From Figs. 5 to 7 it can be seen that the lateral strain is close to zero, but of opposite sign to the axial direct strain, as would have been expected from the Poisson effect. Although the lateral straining remains less than the Poisson value, because of the transverse restraint of the diaphragms, it is considered that the transverse stress as well as strain is sufficiently small to be ignored.

10. Conclusion

The test structure was built to fulfil, as closely as possible, the assumptions of the general theory of Argyris and Dunne. It had, therefore, a moderate and conical taper and was stiffened with closely spaced transverse diaphragms. The thickness of plating prevented buckling, and the structure behaved linearly with load.

An important assumption of the general theory is that both the transverse direct stress and strain are zero. This, though an apparent anomaly is considered justifiable as the results show that both quantities are sufficiently small to have been ignored. As anticipated, the error of the elementary theories is larger for loadings nearer the root. Under the shear loads the maximum direct strains at the root exceeded those computed from the conventional beam theory by up to 20%, and under torque the maximum shear strain immediately inboard of the innermost loading section exceeded that of the Bredt-Batho theory by 3[illegible]%.

The computation for an 'equivalent four boom tube' was comparatively simple and could have been completed in a week, whilst the computation and tabulation of results for the 'tube with direct stress carrying covers' was laborious and required approximately 300 man hours. Both computations gave an equally good estimate of the strains due to torsional loadings. The four boom assumption could not of course interpret the strain lag when shear loads were applied and this was the chief reason

for/

for making the second more complex analysis. Unfortunately the latter has still not done so. It is probable that some estimate of the lag in strain could be obtained by analysing the box as an 'equivalent eight boom tube' having four equally spaced 'booms' across each cover.

The analysis for four boom tubes, because of its relative simplicity, should prove useful in estimating the stresses due to torsion of tubes with quadrilateral cross sections. It seems reasonable to state that the accuracy will be higher when corner booms are present though some experimental confirmation of this is desirable.

Acknowledgements

The author is indebted to Prof. A. J. S. Pippard and Dr. S. R. Sparkes of the Imperial College of Science and Technology for the opportunity and facilities for doing the work and for help and encouragement during its progress.

He also wishes to record his gratitude to the Ministry of Supply for providing the test box, to the Department of Scientific and Industrial Research for a grant covering the test frame and assistance, to Mr. T. P. H. George and others of the Fairey Aviation Company for help during manufacture of the test box and components of the loading linkage, to the Director of the Royal Aircraft Establishment for the loan of electrical strain measuring equipment and to Mr. C. P. G. Bateman and Mr. J. Neale for assistance in planning and testing. Mrs. B. H. Falconer did much of the curve-plotting, and Miss E. Horton made many of the detailed computations.

Finally thanks are due to Dr. J. C. Chapman for numerous invaluable discussions during the course of the project.

15 128
Plate 1

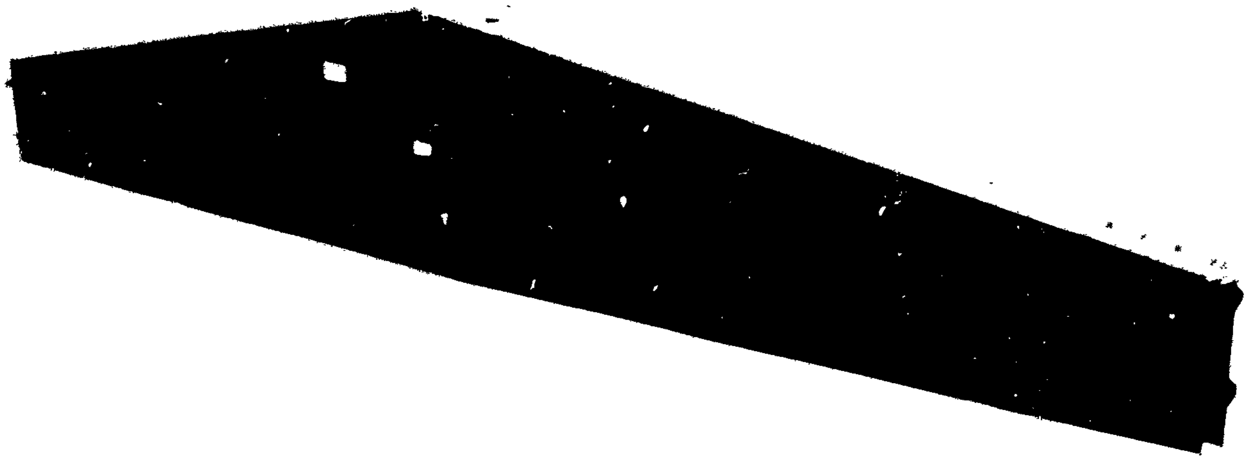

The Tapered Test Box

16,128
Plate 2

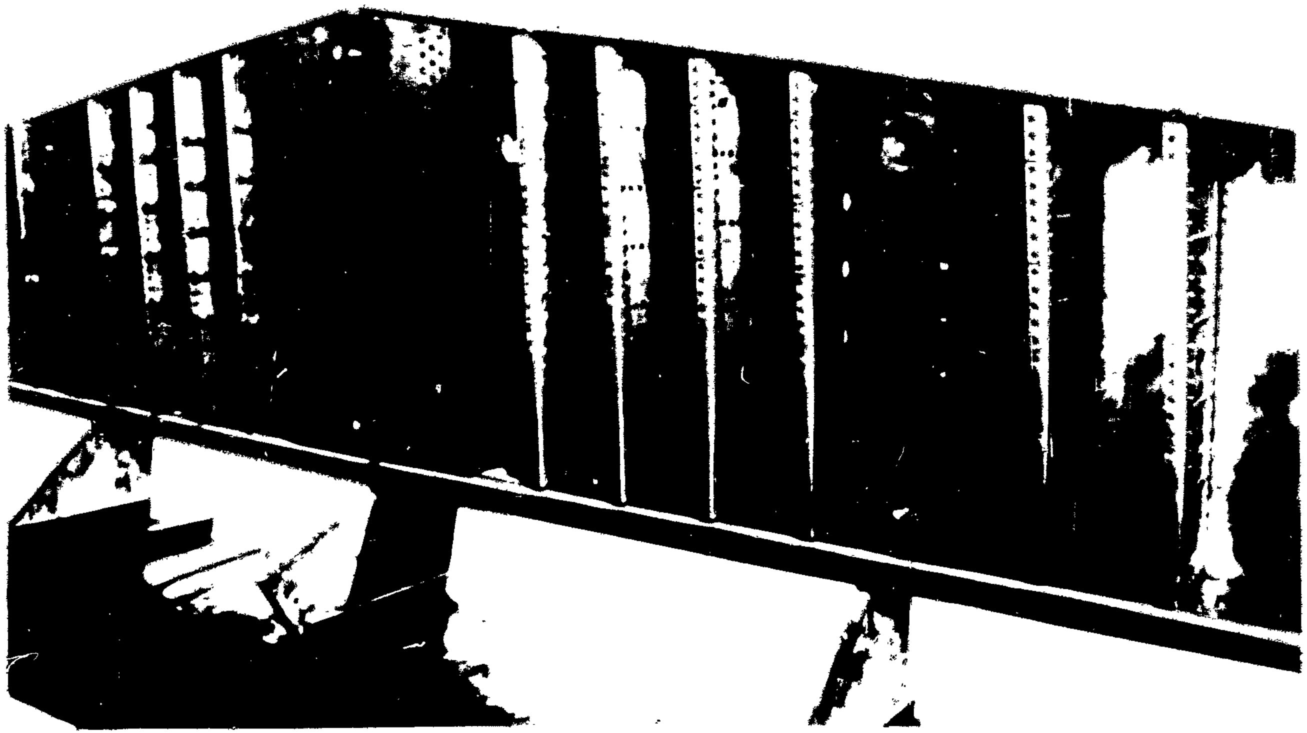

Details of the Internal Construction of the Box

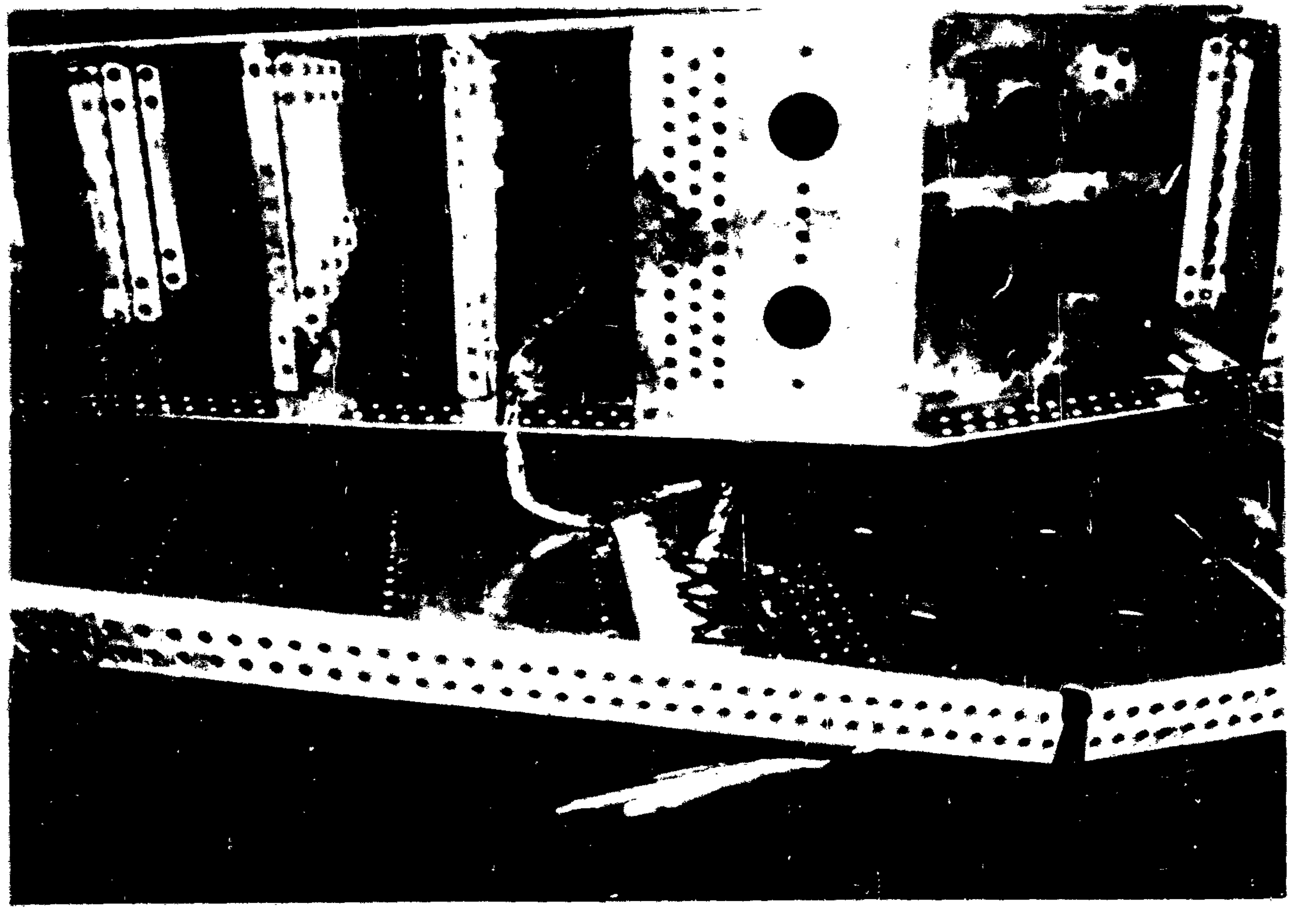

Details of the Internal Construction of the Box

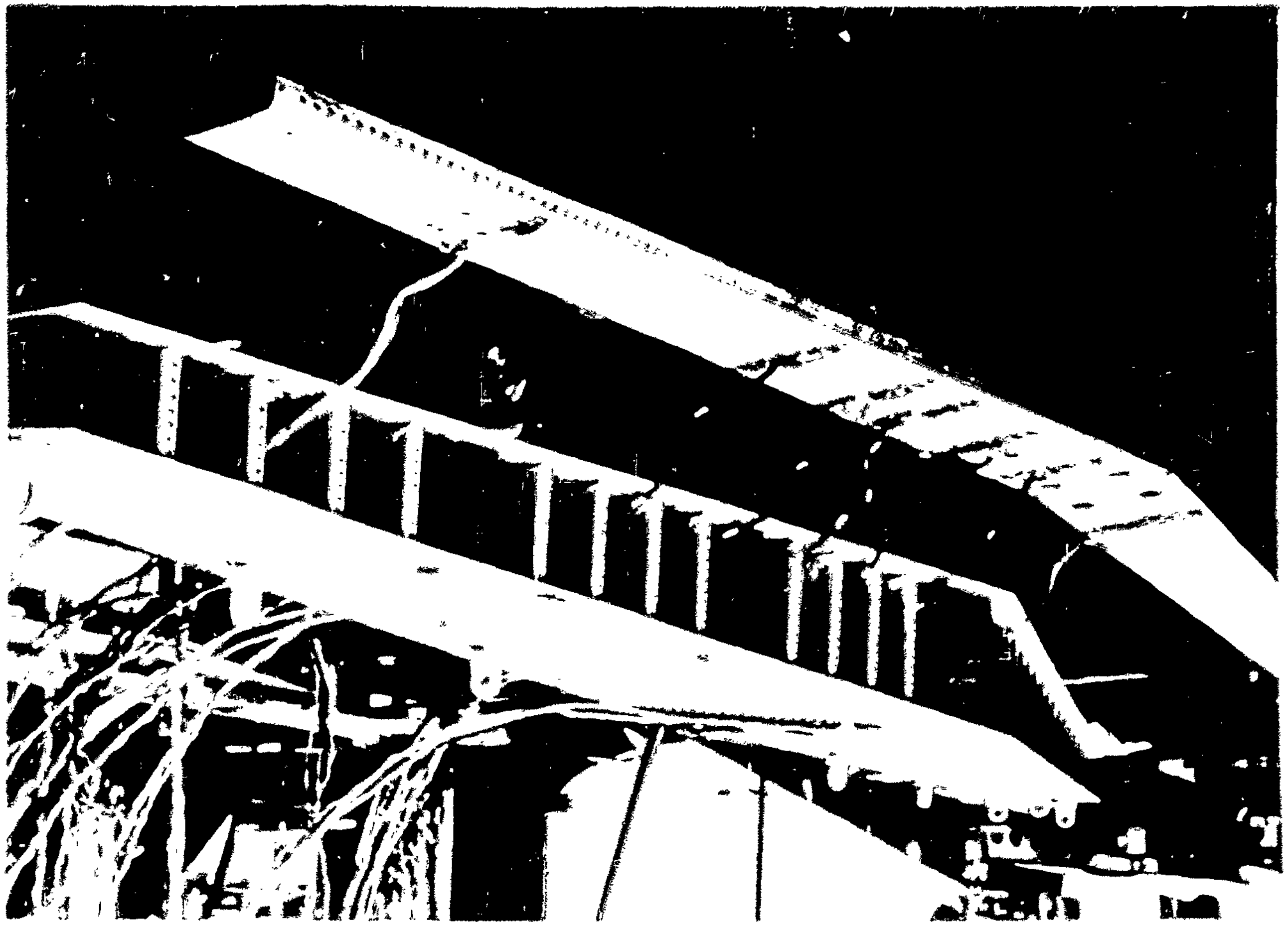

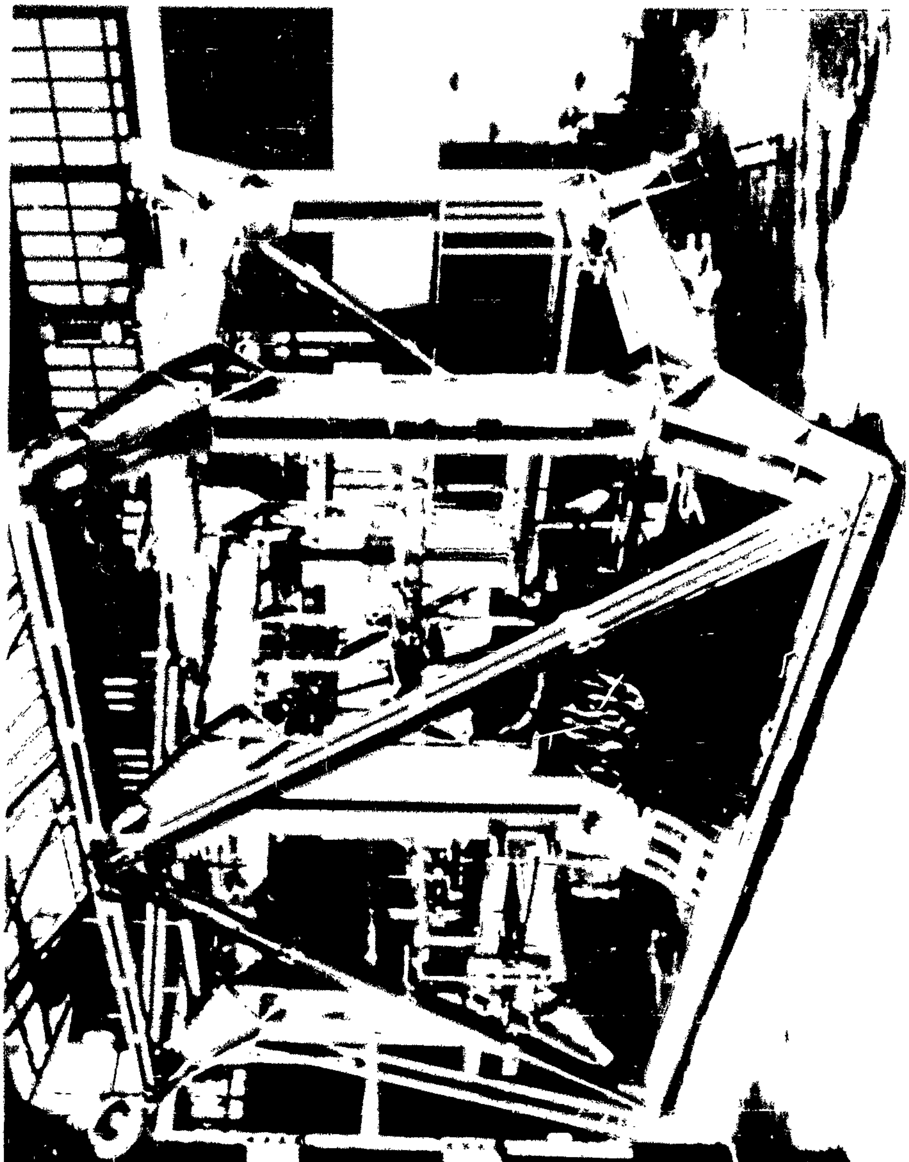

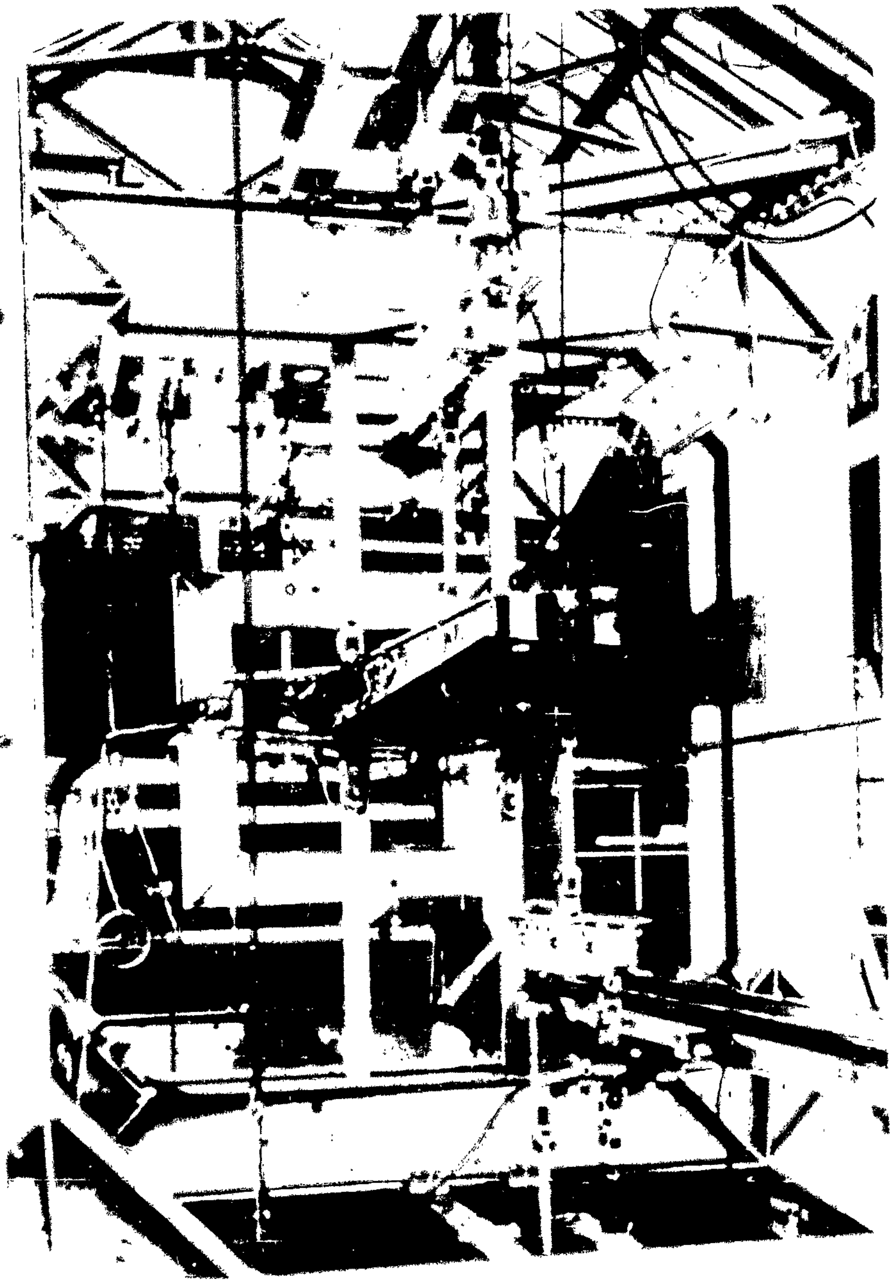

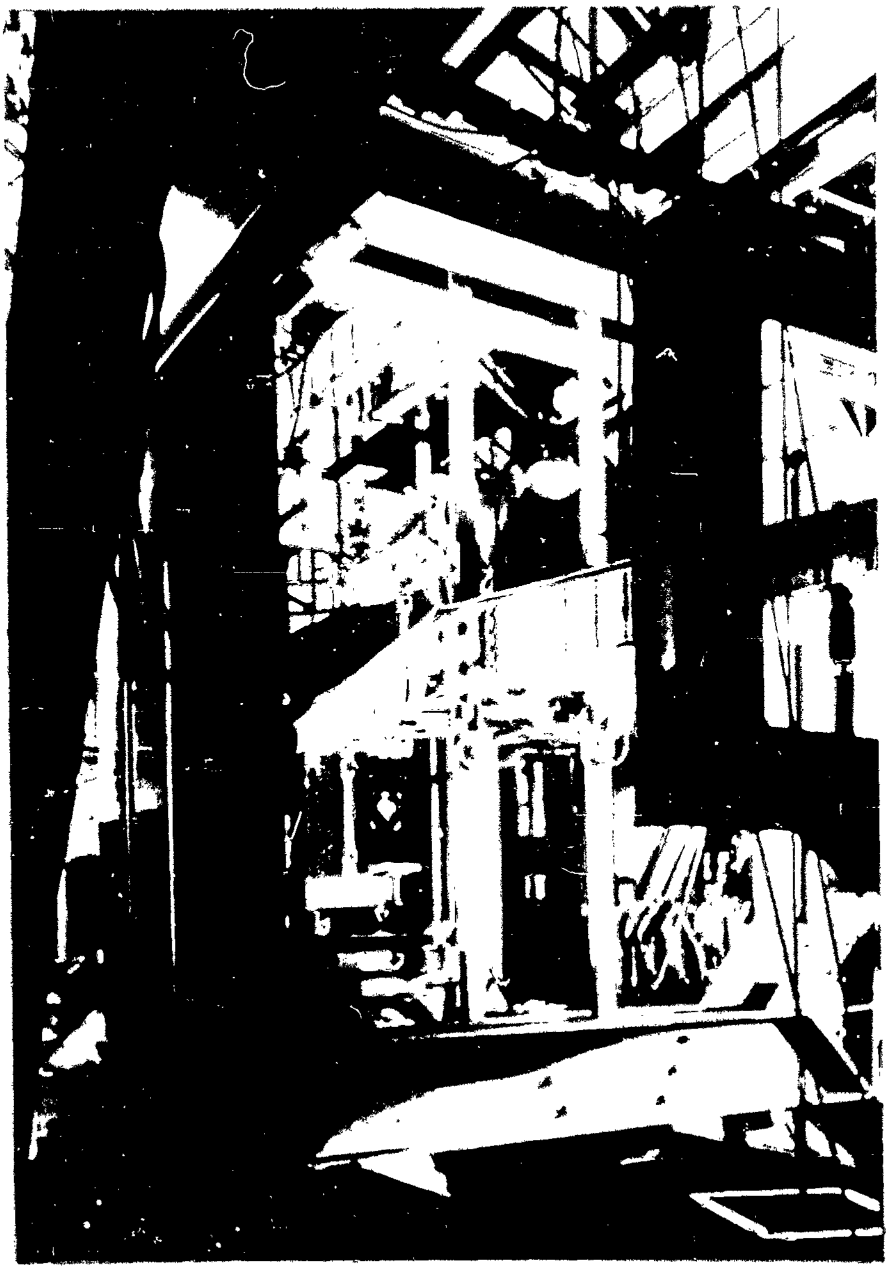

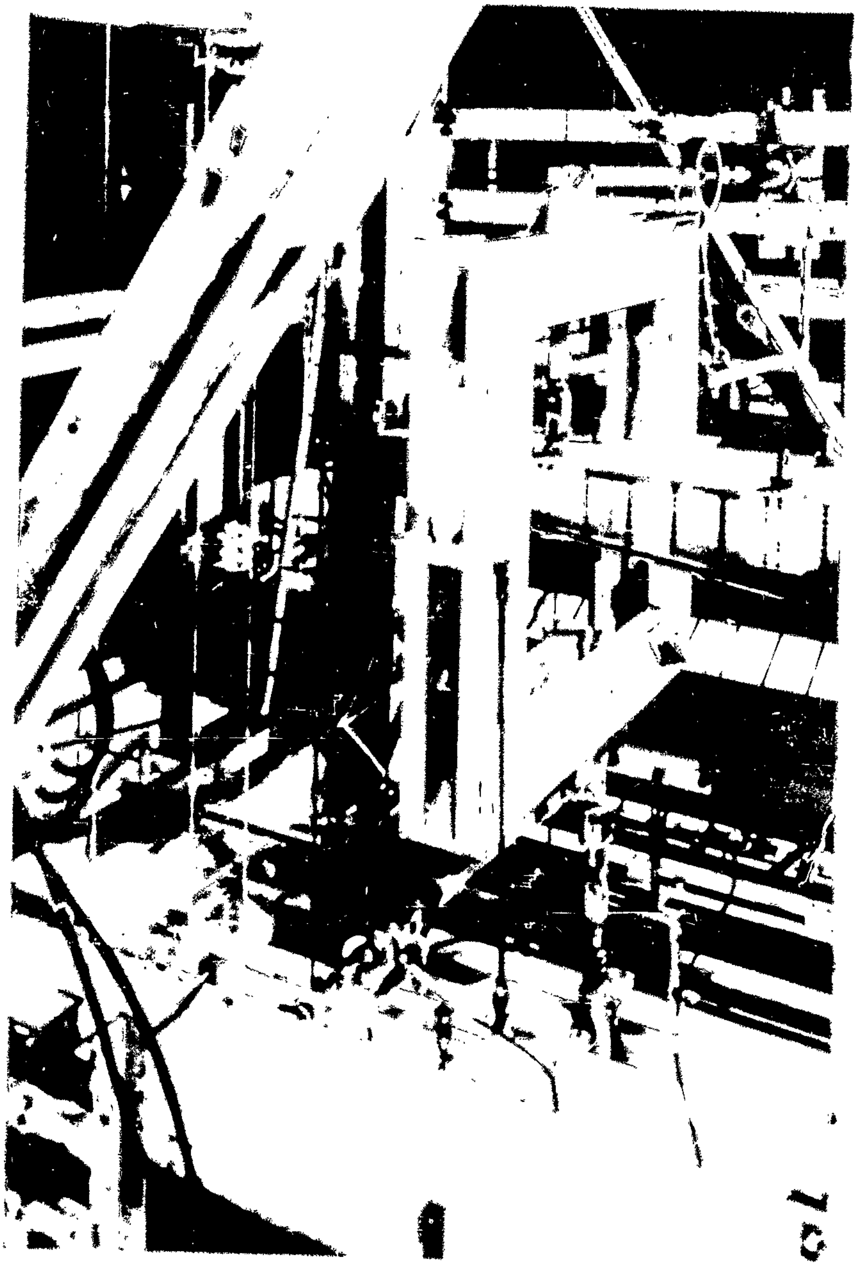

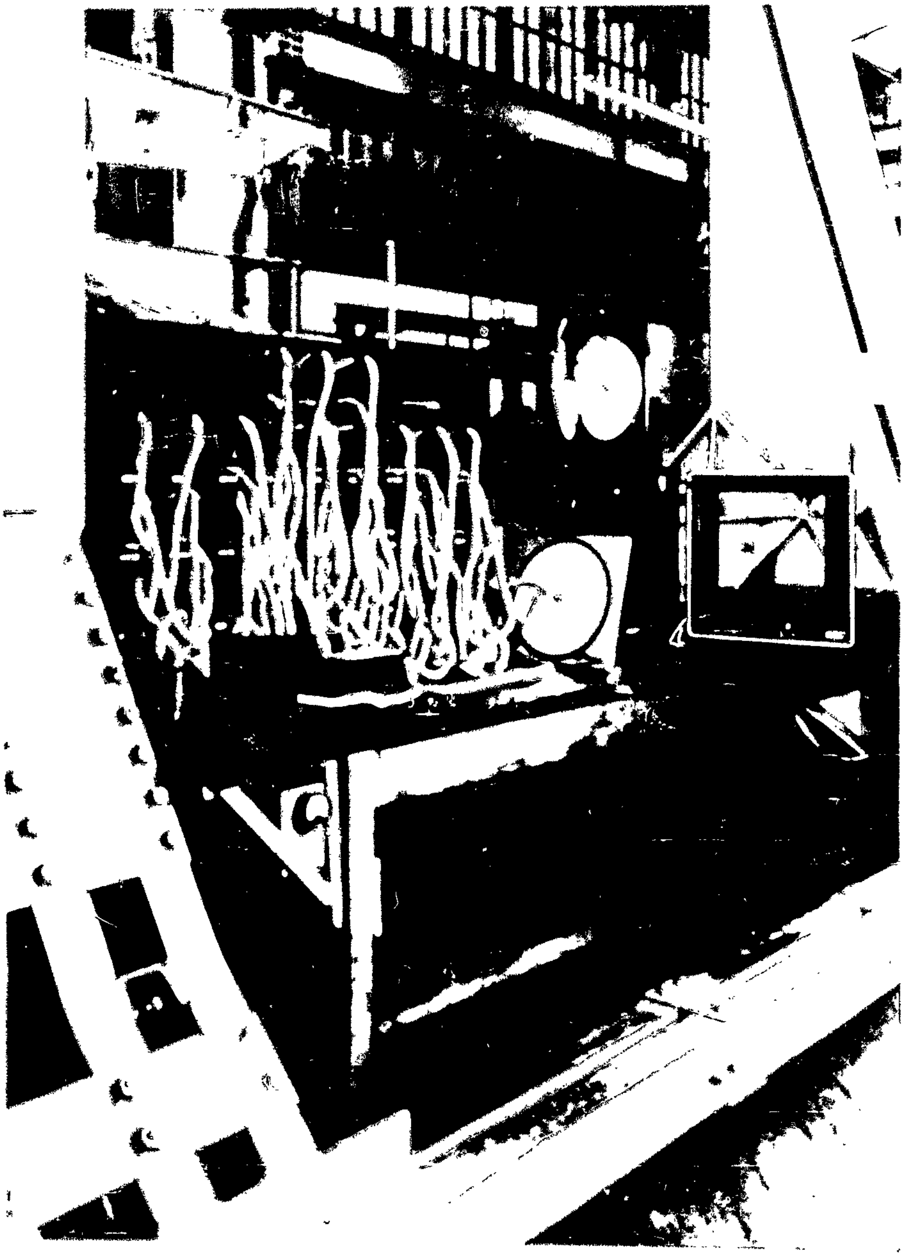

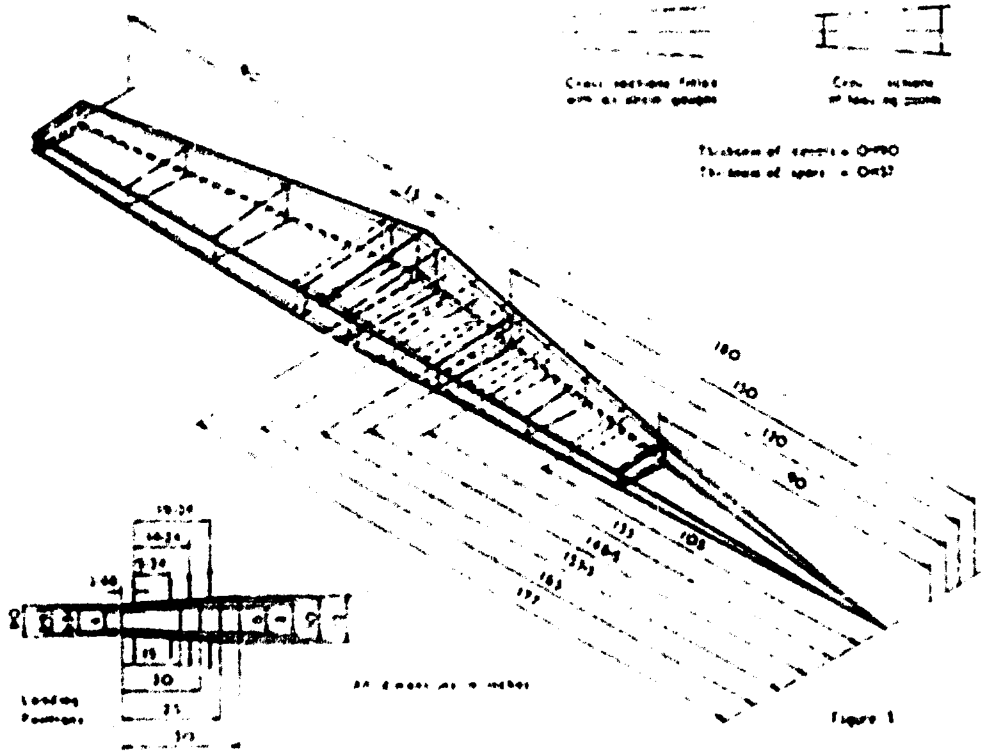

Figure 1

ISOMETRIC DIAGRAM OF THE TAPERED BOX

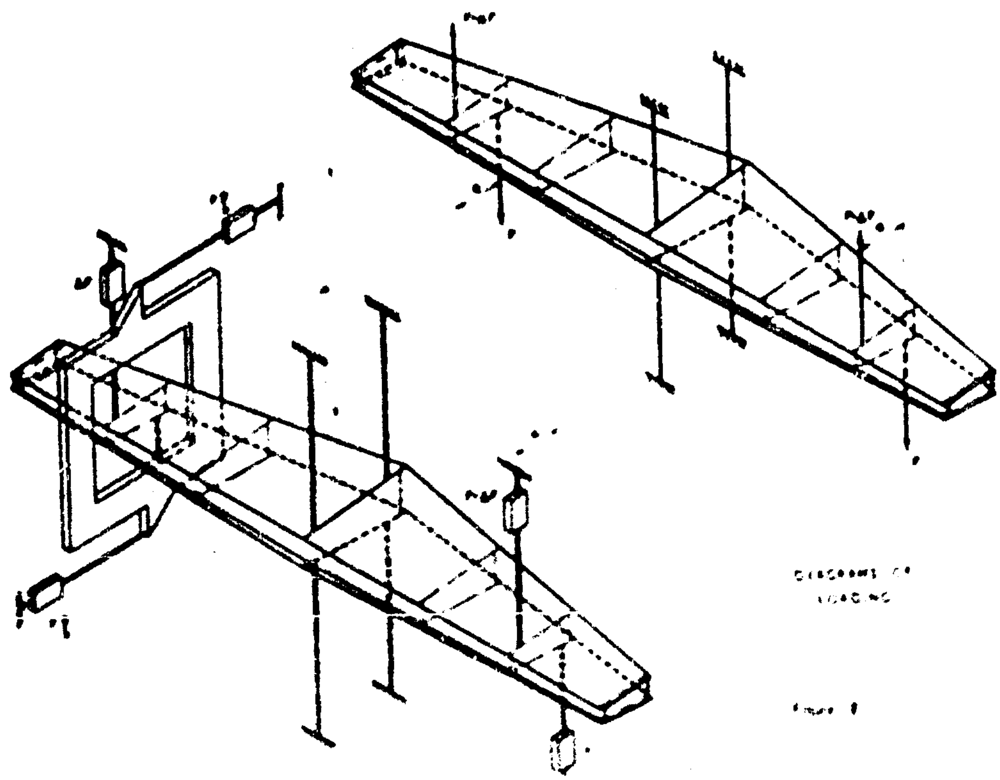

DIAGRAMS OF LOADING

Figure 2

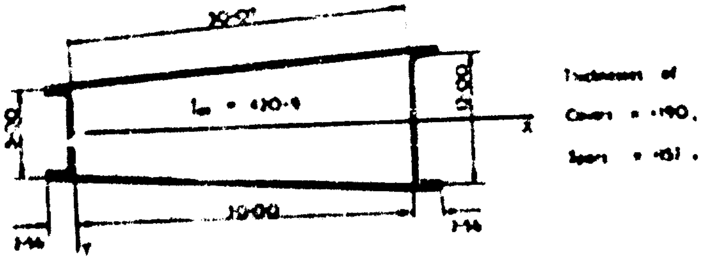

ACTUAL ROOT CROSS SECTION. (a)

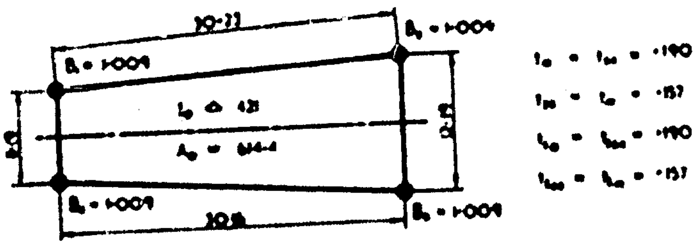

SECTION FOR ELEMENTARY THEORIES (b)

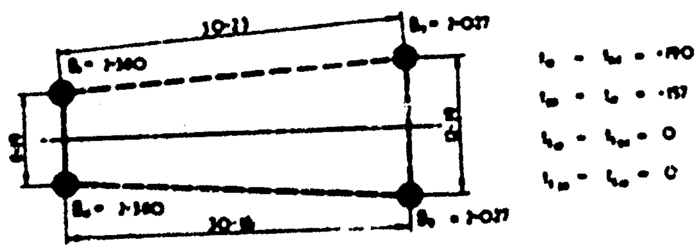

THE EQUIVALENT FOUR BOOM TUBE. (c)

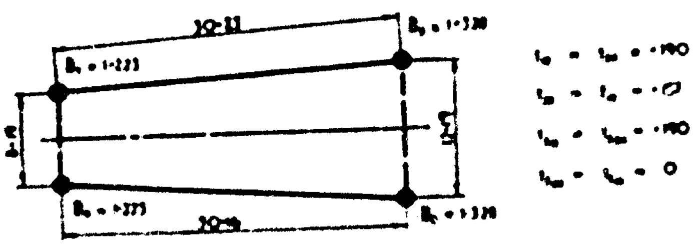

WHEN COVERS CARRY DIRECT STRESS (d)

ROOT CROSS SECTION DIMENSIONS USED IN COMPUTATION

(All dimensions in inches) Figure 3

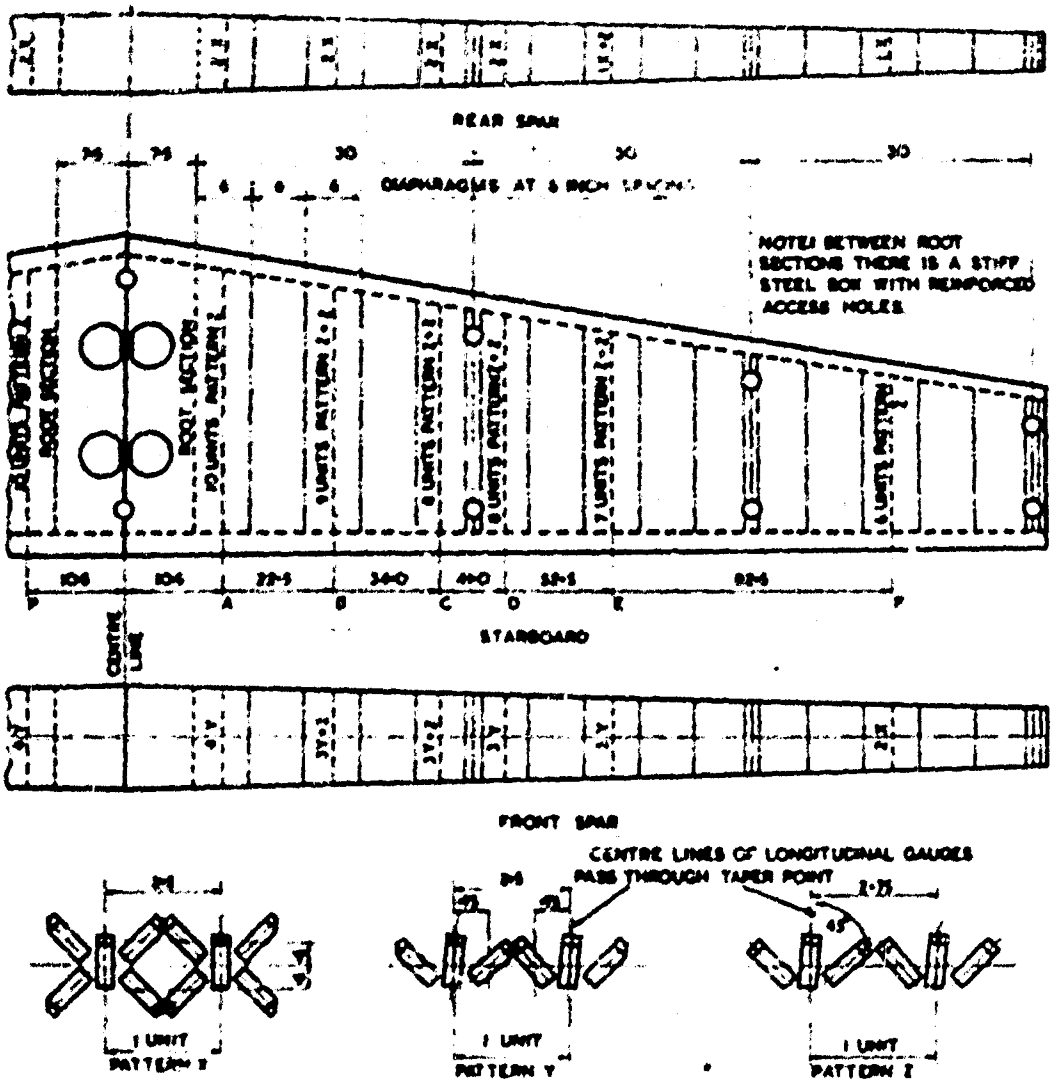

ALL DIMENSIONS IN INCHES.

TINSLEY 6K 100 OHM ELECTRICAL RESISTANCE STRAIN GAUGES USED ON INSIDE AND OUTSIDE OF BOX

SECTION	P	A	B	C	D	E	F	TOTAL
LONGITUDINAL	60	60	66	62	38	56	38	400
INCLINED	112	112	100	92	92	76	72	656
TOTAL	172	172	166	154	130	132	110	1056

DISTRIBUTION

ARRANGEMENT OF STRAIN GAUGES FOR TAPERED BOX.

Figure 4

TB 94

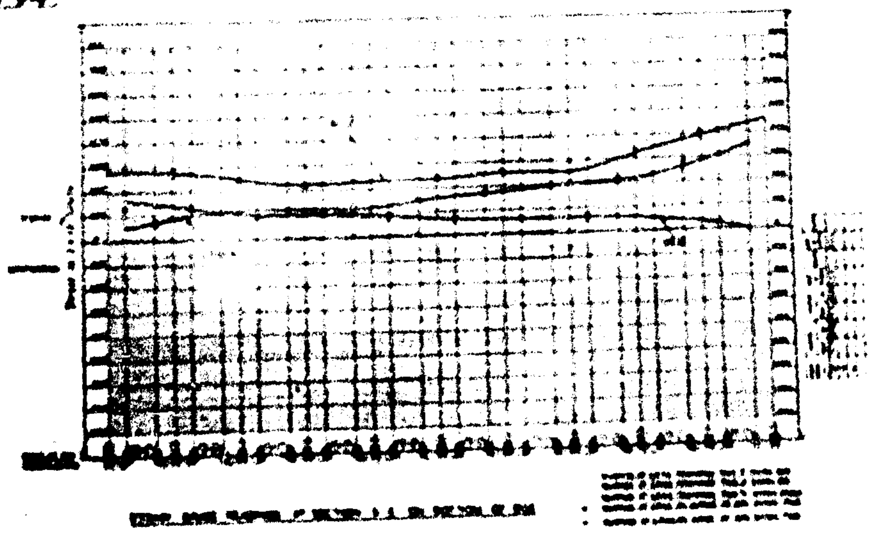

TB 94

TB 95

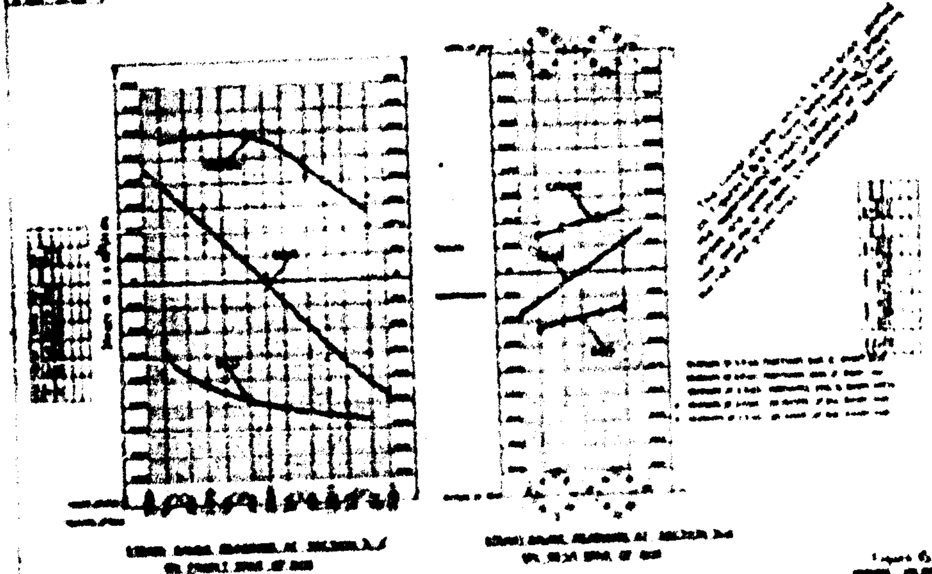

TB 95

TB 93

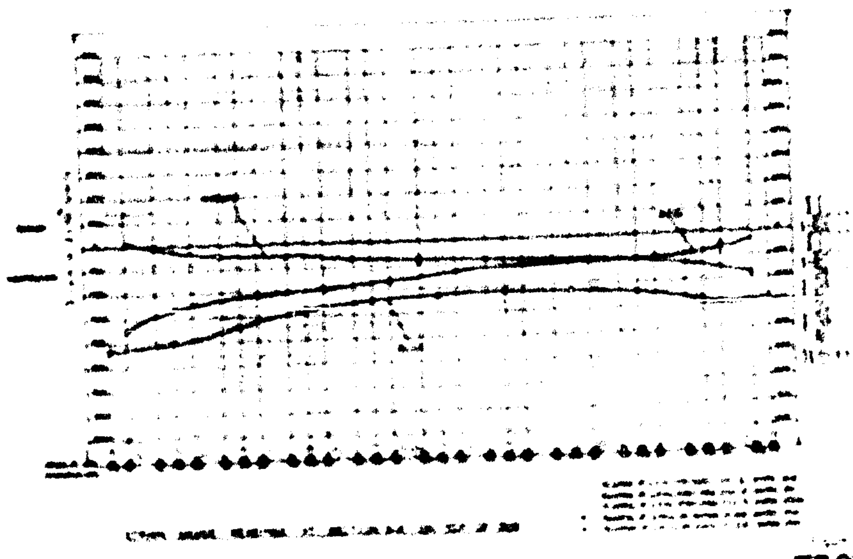

TB 93

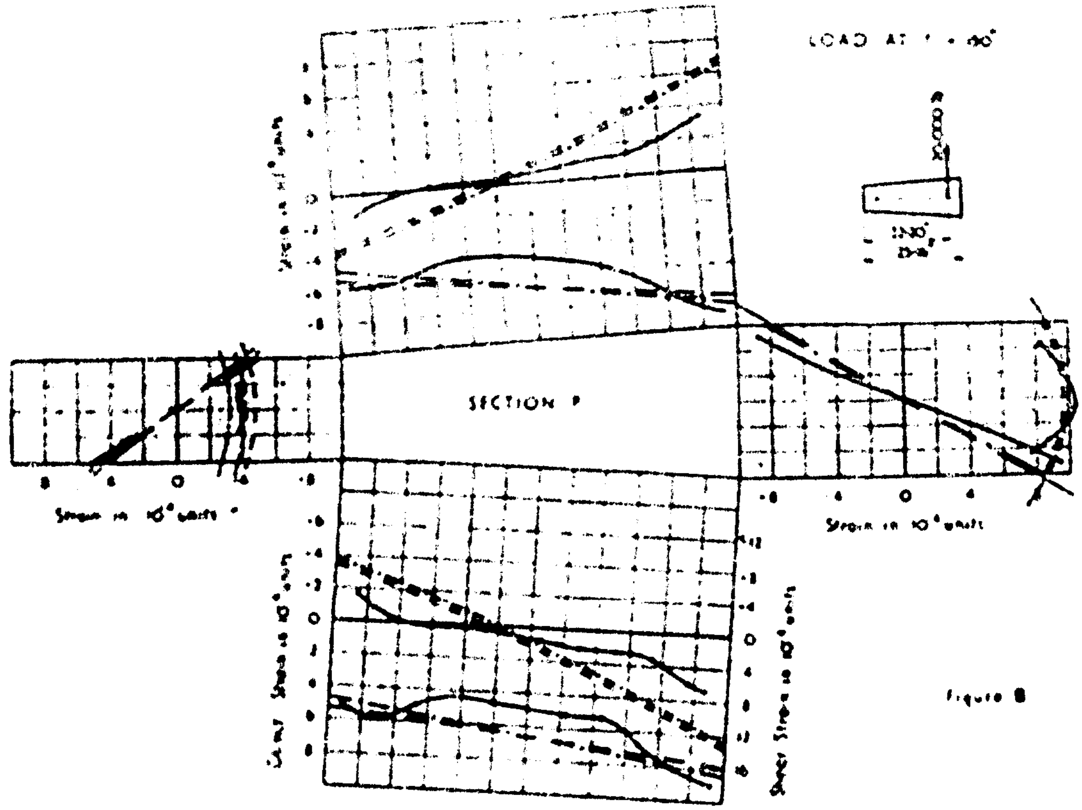

Figure 8

	Direct Strain	Shear Strain
Experiment		
Elementary Theory		
Equivalent four boom tube		
Covers carrying direct stress		

Tensile strains and anticlockwise shear strains are considered positive and are plotted outwards. The direct strains are drawn full scale and the shear strains half scale.

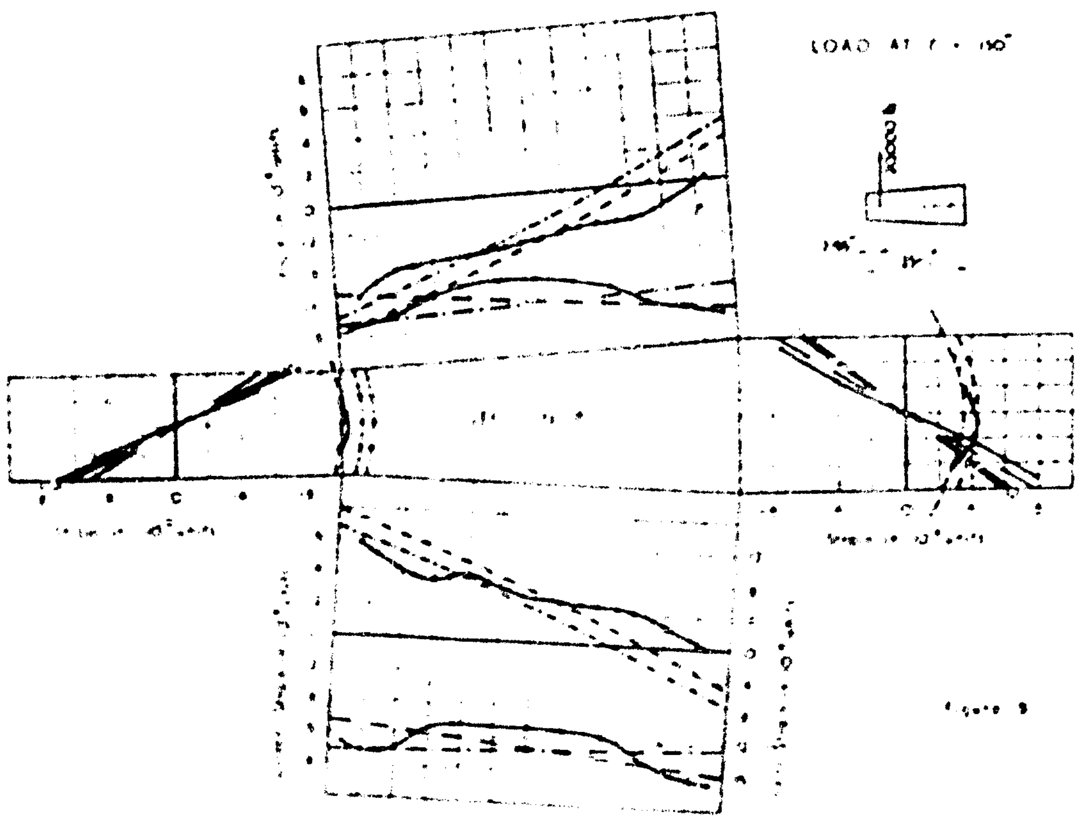

Figure 9

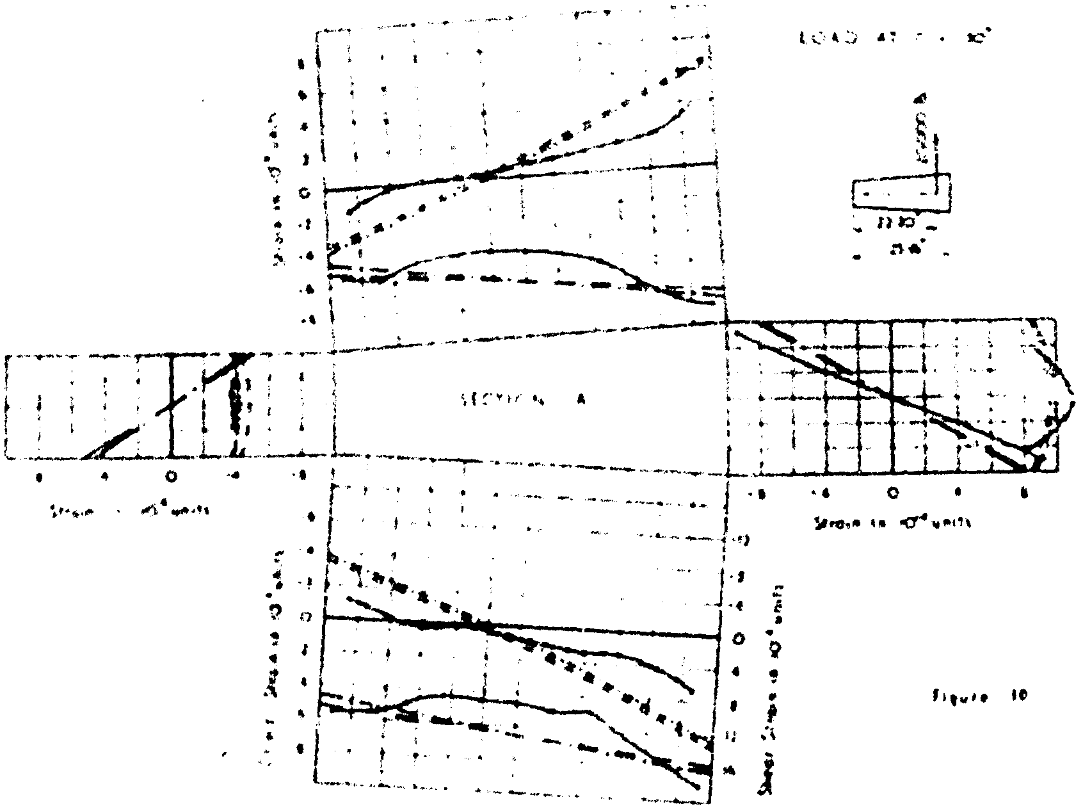

Figure 10

	Direct Strain	Shear Strain
Experiment	————	—·—·——
Elementary Theory	— — —	- - - - - -
Equivalent four boom tube	—·—·—	-·-·-·-

Tensile strains and anticlockwise shear strains are considered positive and are plotted outwards. The direct strains are drawn full scale and the shear strains half scale.

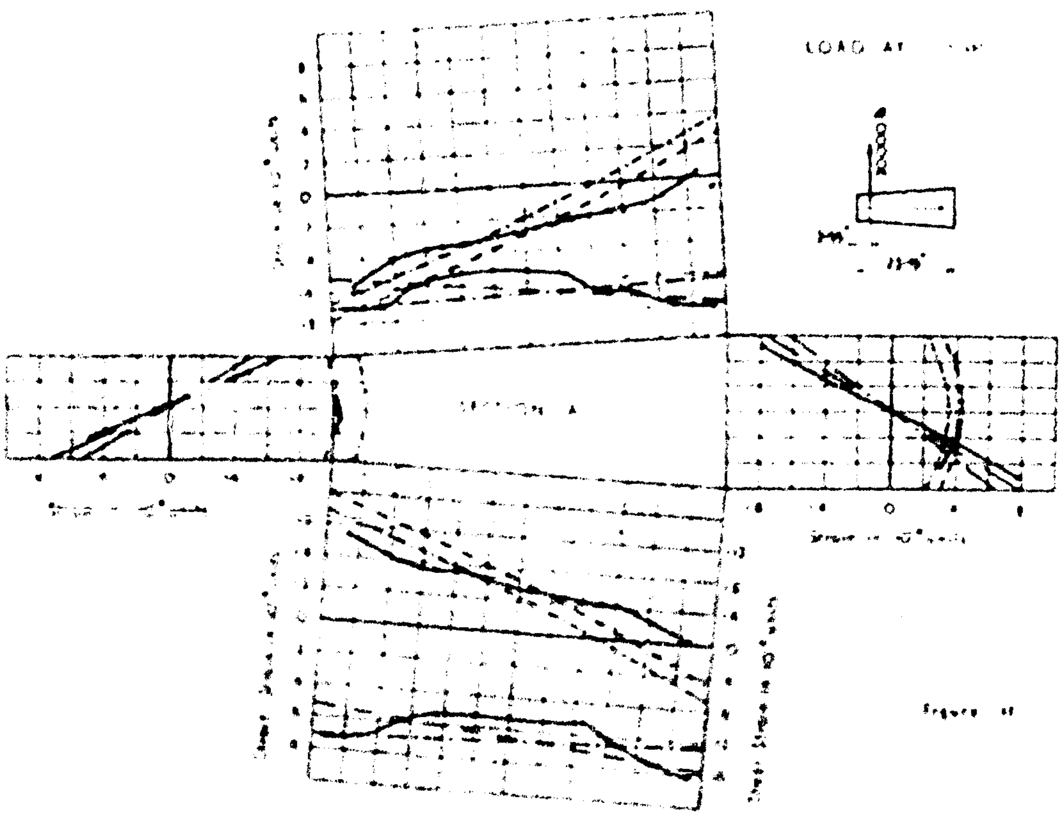

Figure 11

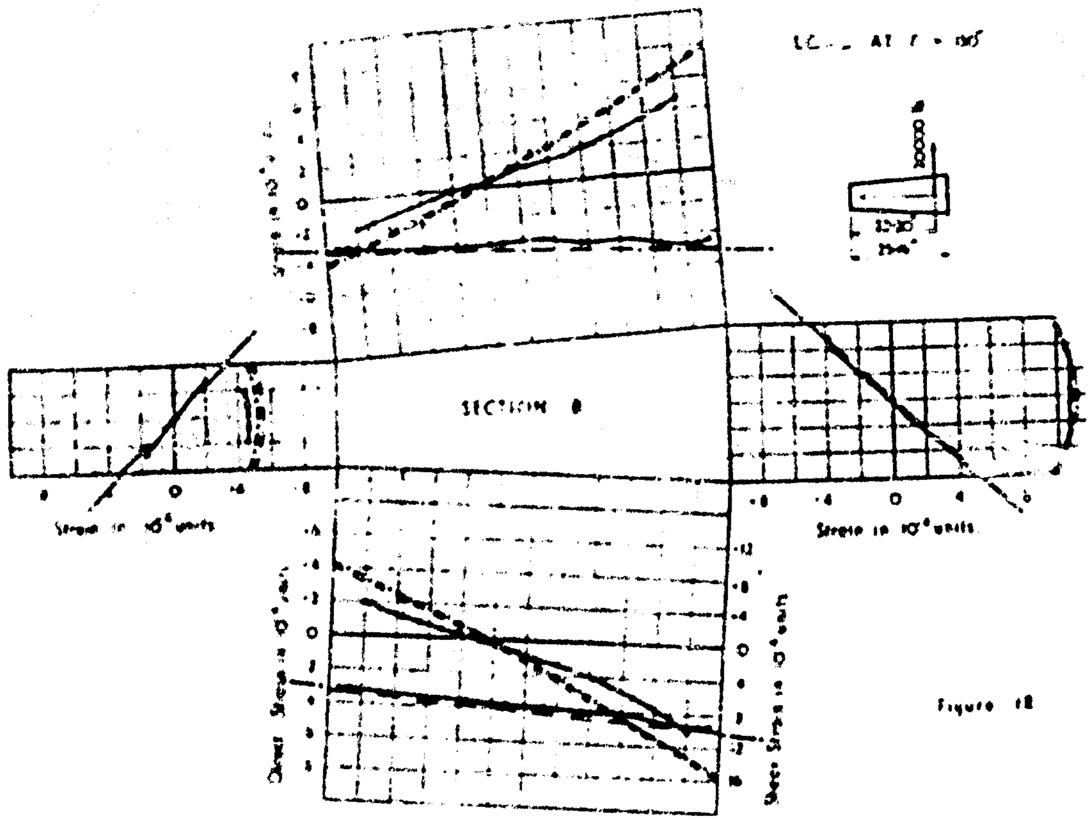

Figure 18

	Direct Strain	Shear Strain
Experiment		
Elementary Theory		
Equivalent four boom tube		

Tensile stress and anticlockwise shear stress are considered positive and are plotted outwards. The direct stresses are drawn full scale and the shear stresses half scale.

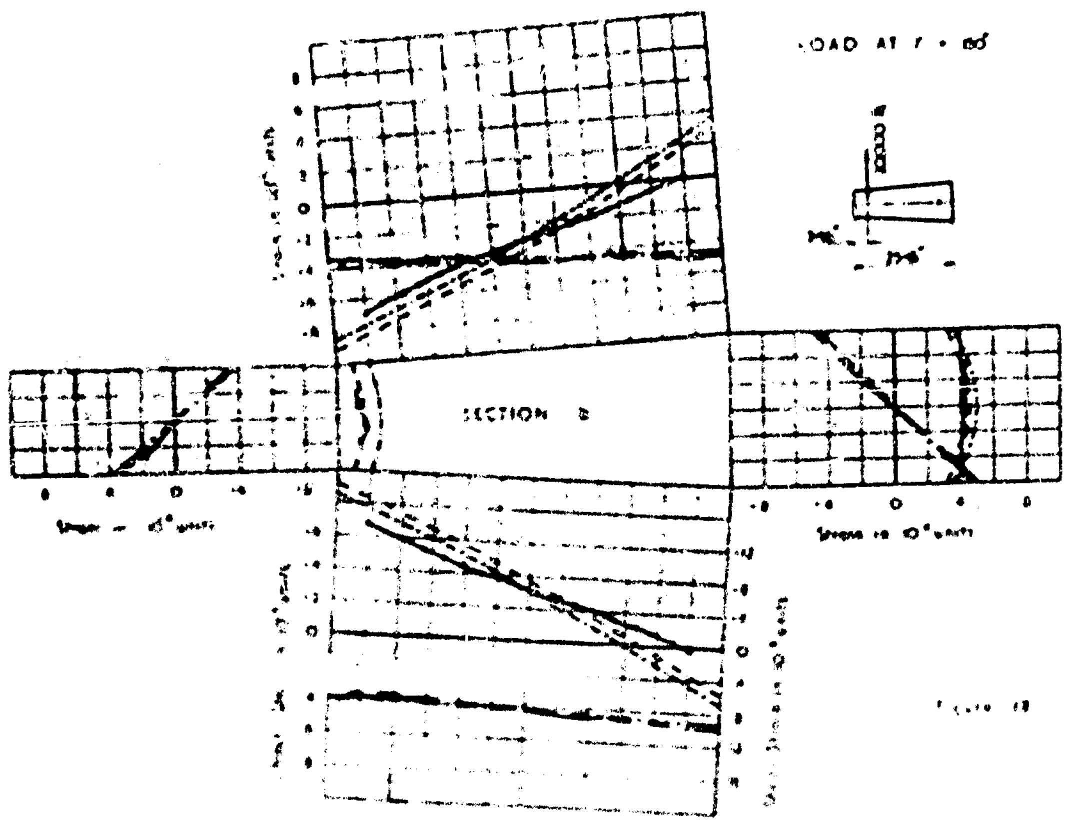

Figure 18

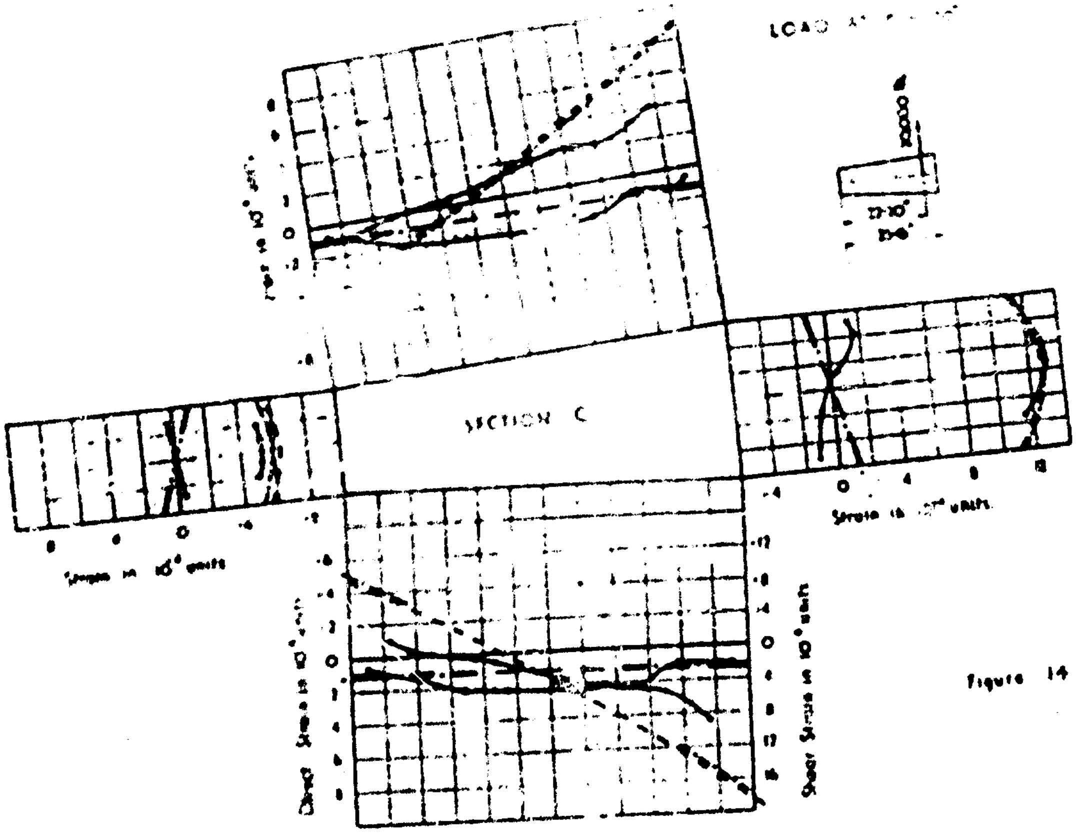

Figure 14

	Direct Strain	Shear Strain
Experiment	———	———
Elementary Theory	— — —	- - - - - -
'Equivalent four beam tube'	—·—·—	-·-·-·-

Tensile strains and anticlockwise shear strains are considered positive and are plotted outwards. The direct strains are drawn full scale and the shear strains half scale.

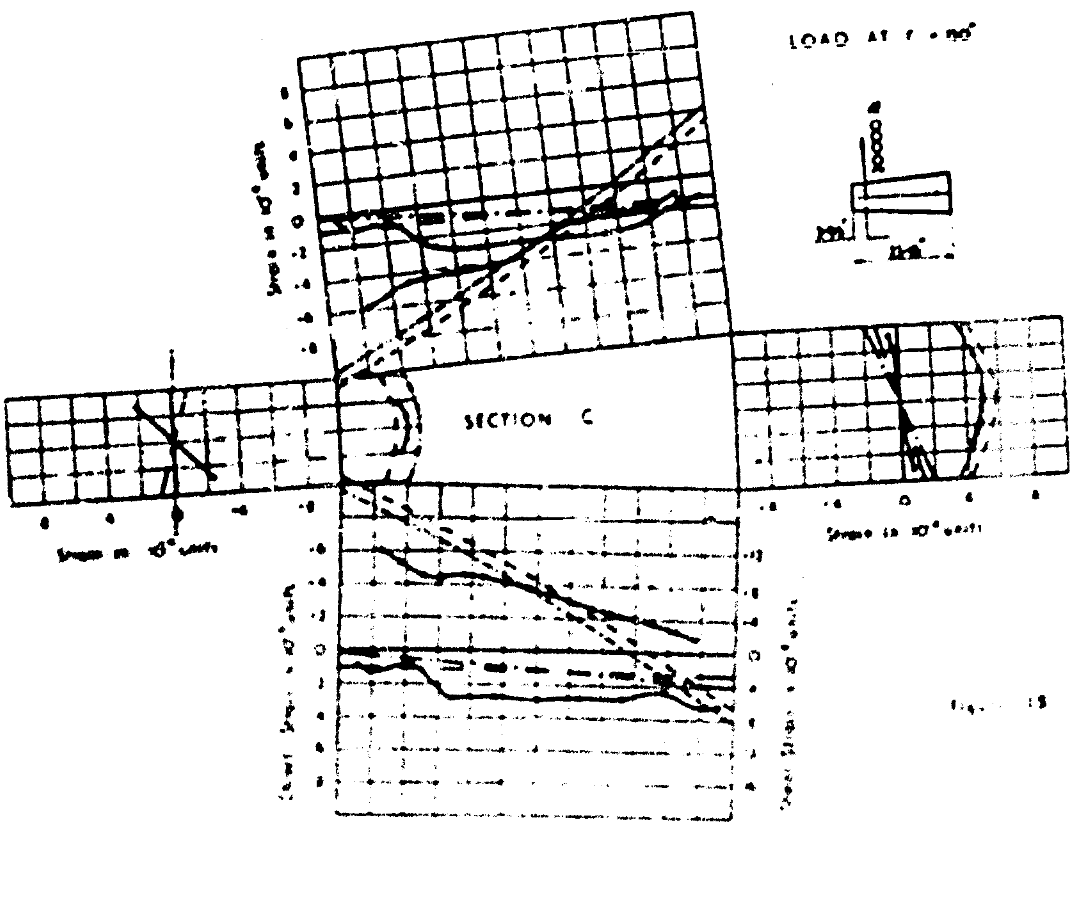

Figure 15

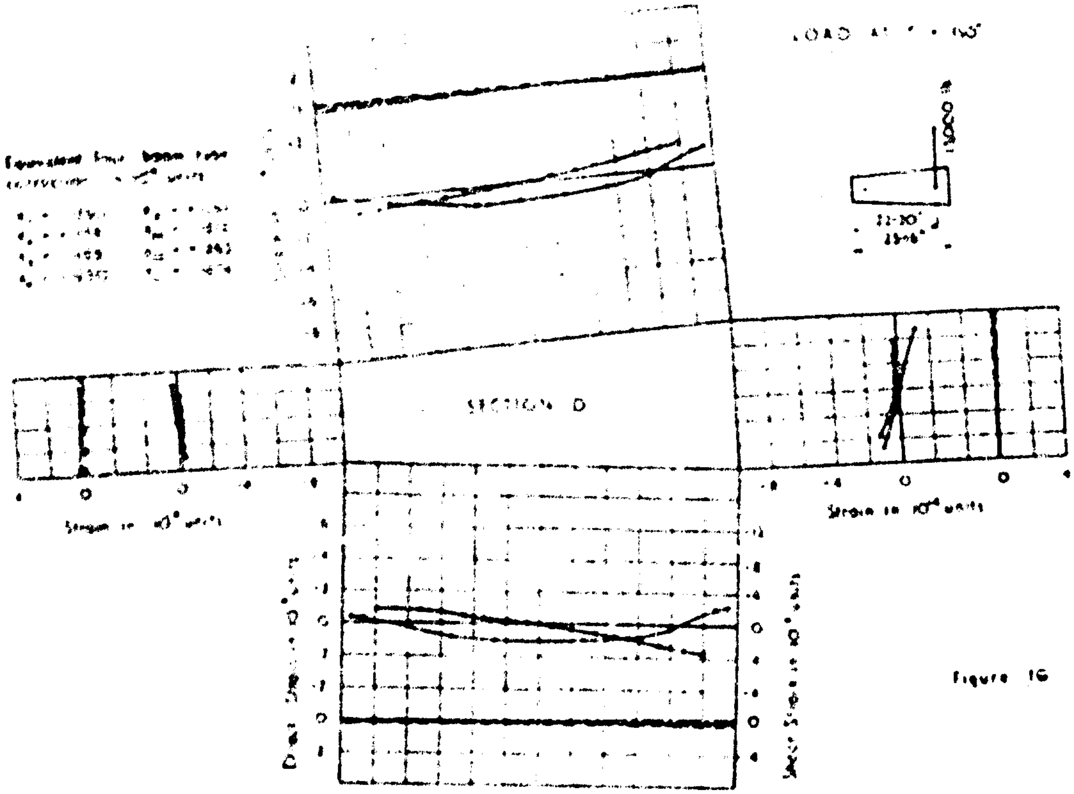

Figure 16

	Direct Strain	Shear Strain
Experiment		
Elementary Theory		
Equivalent four boom tube		

Tensile strains and anticlockwise shear strains are considered positive and are plotted outwards. The direct strains are drawn full scale and the shear strains half scale.

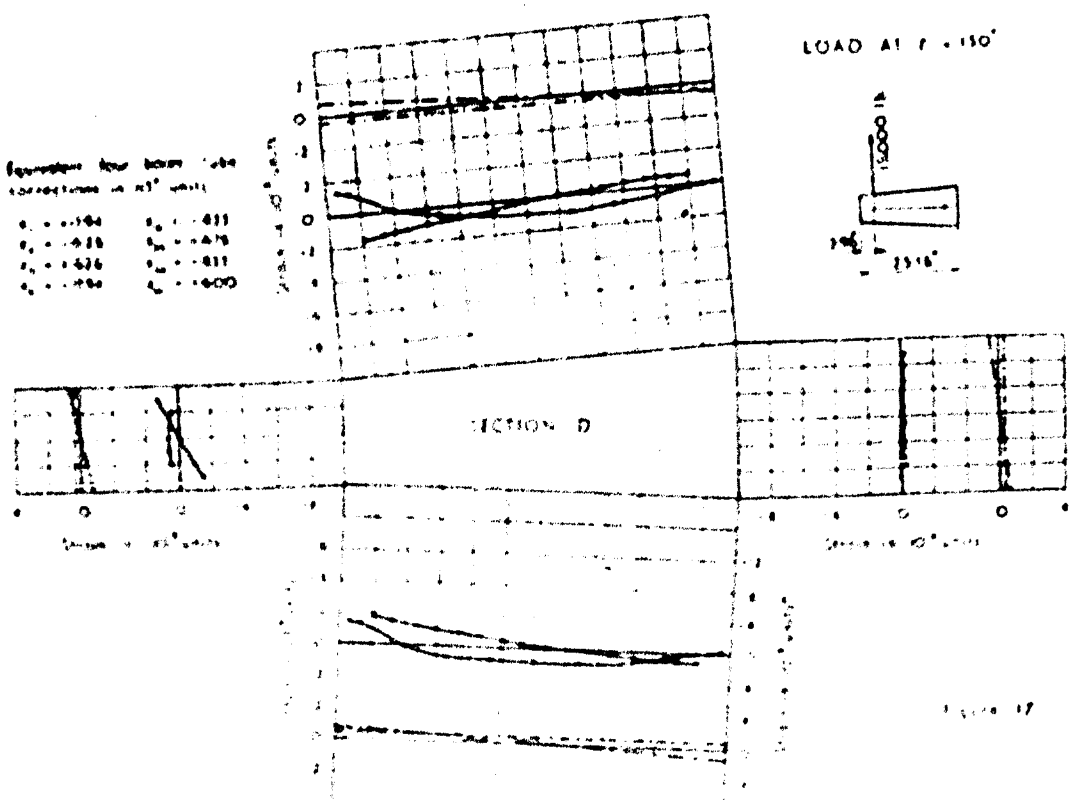

Figure 17

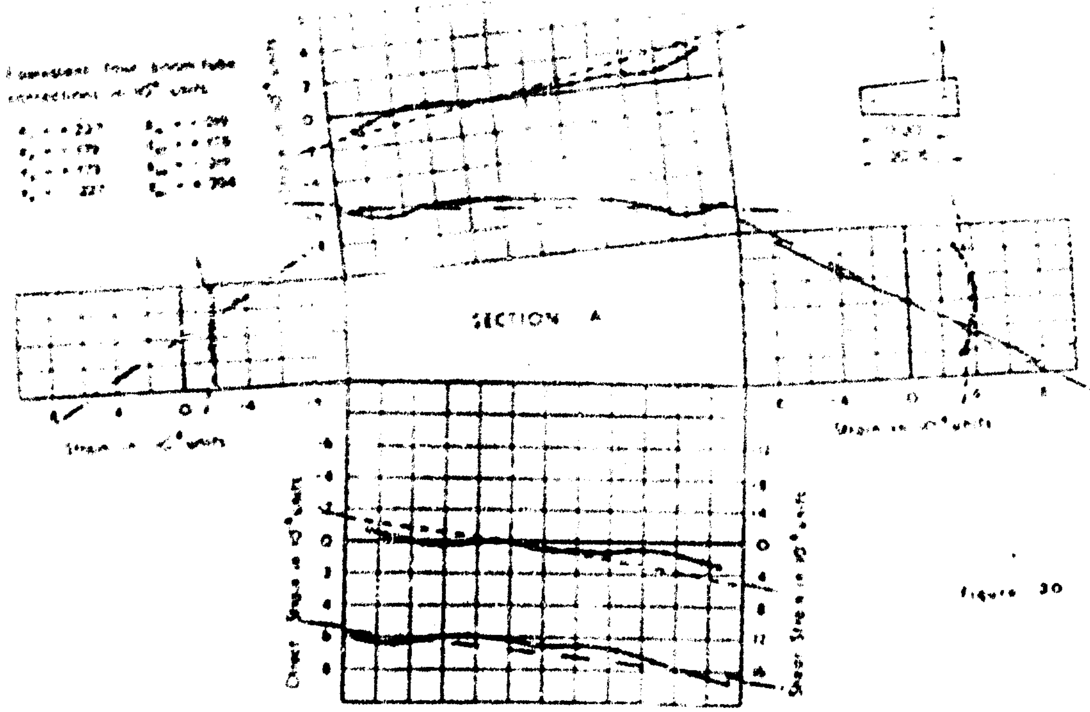

Figure 30

Direct Strain   Shear Strain

Experiment

Elementary Theory

Equivalent four boom tube

Tensile strains and anticlockwise shear strains are considered positive and are plotted outwards. The direct strains are drawn full scale and the shear strains half scale.

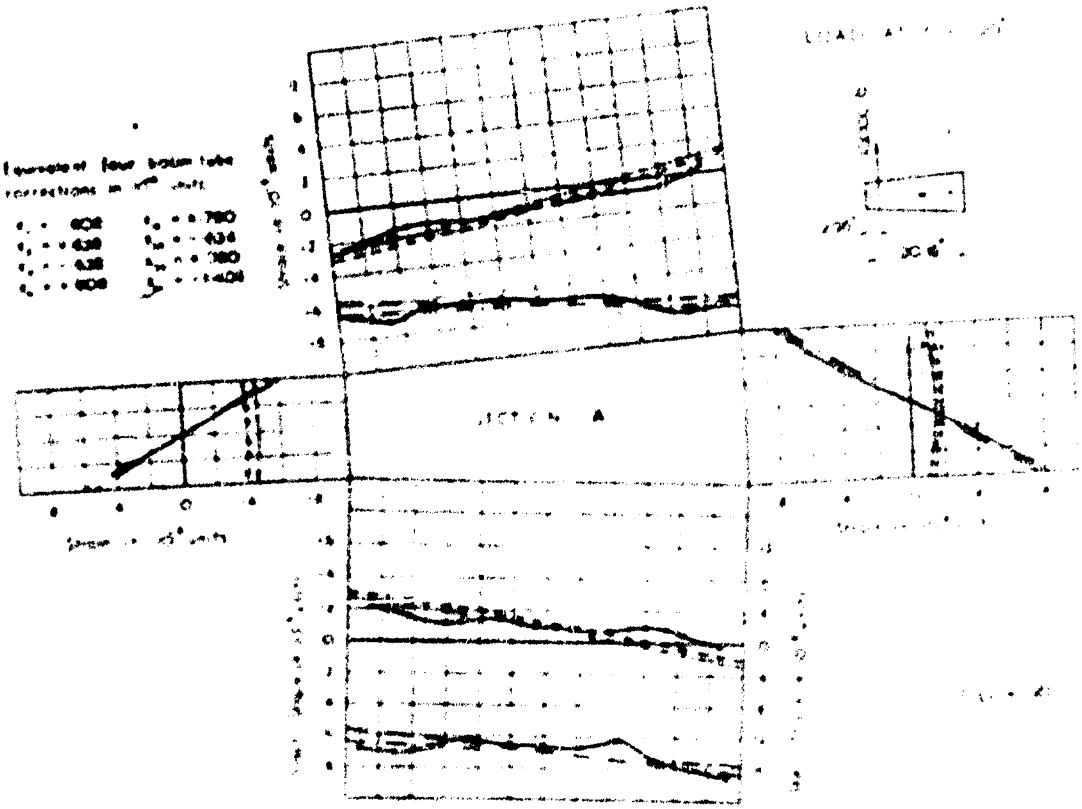

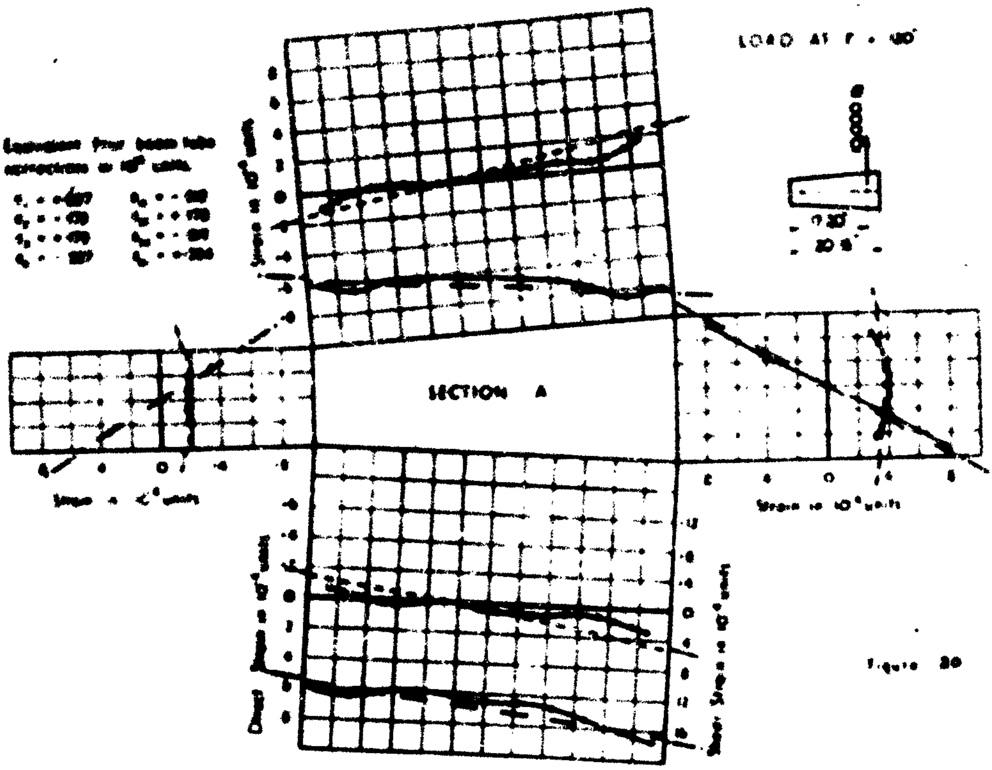

Figure 20

	Direct Strain	Shear Strain
Experiment		
Elementary Theory		
Equivalent four beam tube		

Tensile strains and anticlockwise shear strains are considered positive and are plotted outwards. The direct strains are drawn full scale and the shear strains half scale.

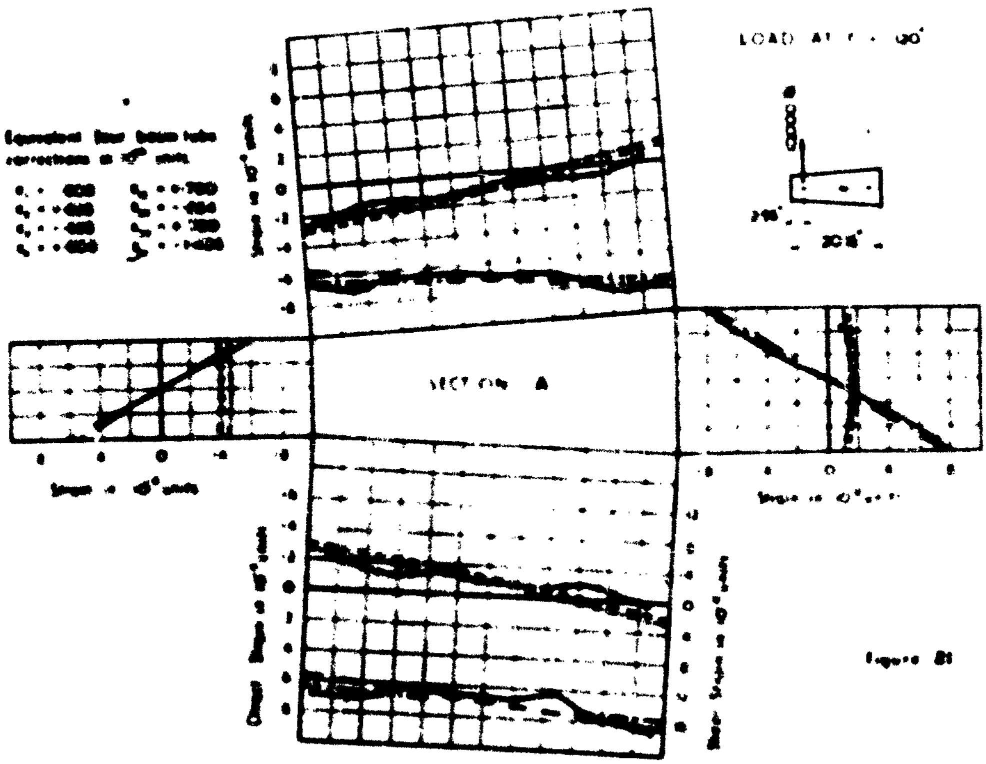

Figure 21

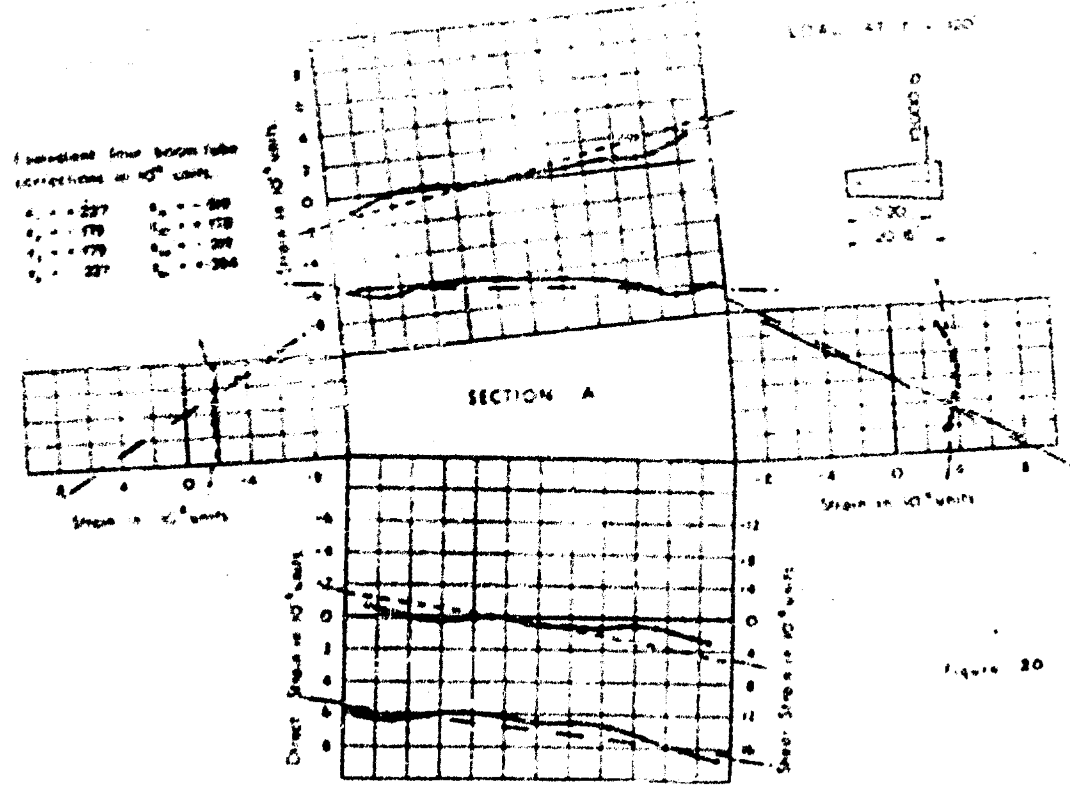

Figure 20

	Direct Strain	Shear Strain
Experiment		
Elementary Theory		
Equivalent four boom tube		

Tensile strains and anticlockwise shear strains are considered positive and are plotted outwards. The direct strains are drawn full scale and the shear strains half scale.

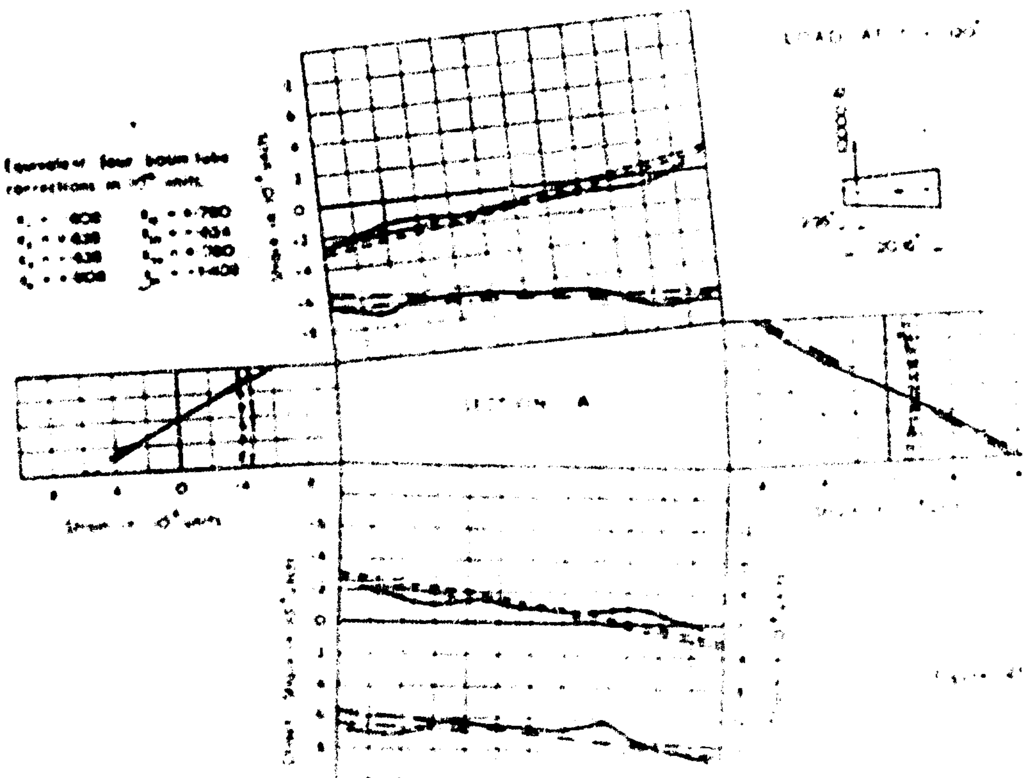

Figure 21

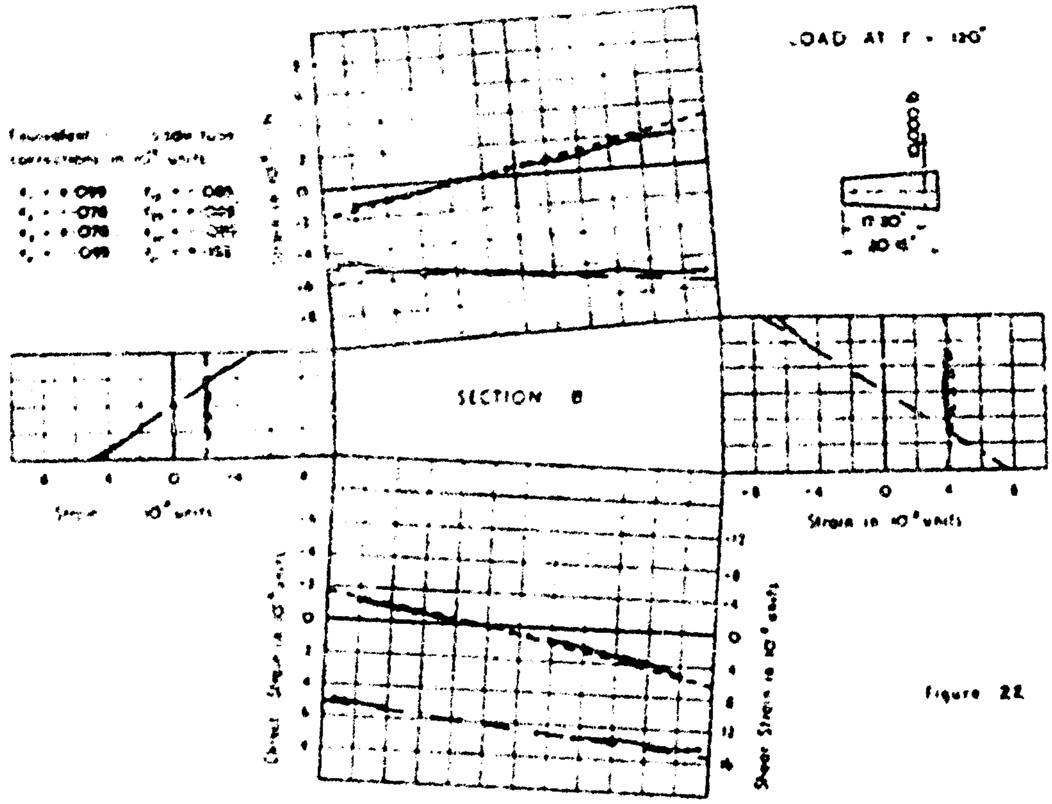

Figure 22

	Direct Strain	Shear Strain
Experiment	————	————
Elementary Theory	— — —	- - - - -
Equivalent four boom tube'	—·—·—	-·-·-·-·

Tensile strains and anticlockwise shear strains are considered positive and are plotted outwards. The direct strains are drawn full scale and the shear strains half scale.

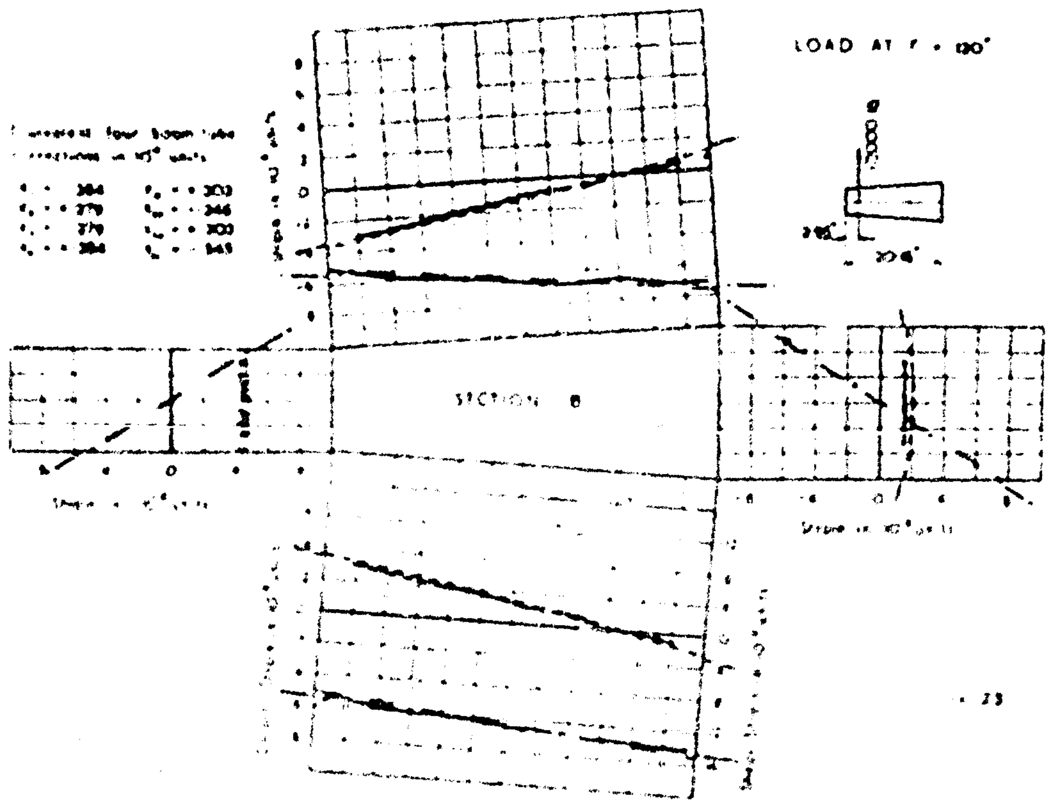

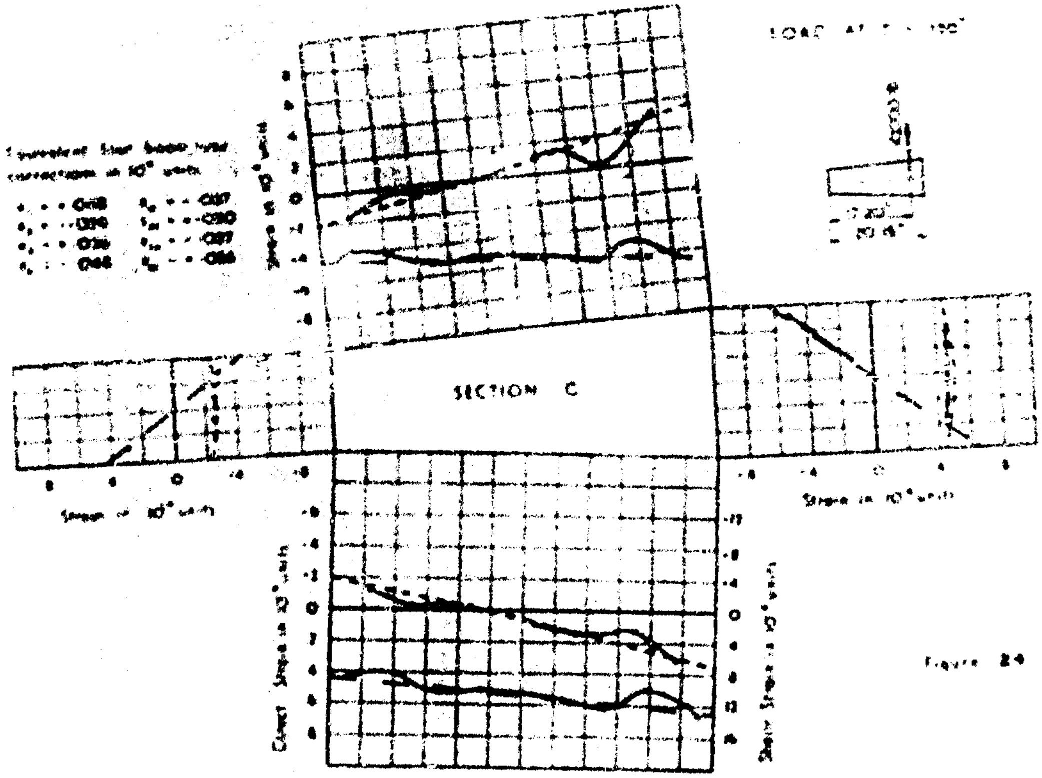

Figure 24

	Direct Strain	Shear Strain
Experiment		
Elementary Theory		

Tensile strains and anticlockwise shear strains are considered positive and are plotted outwards. The direct strains are drawn full scale and the shear strains half scale.

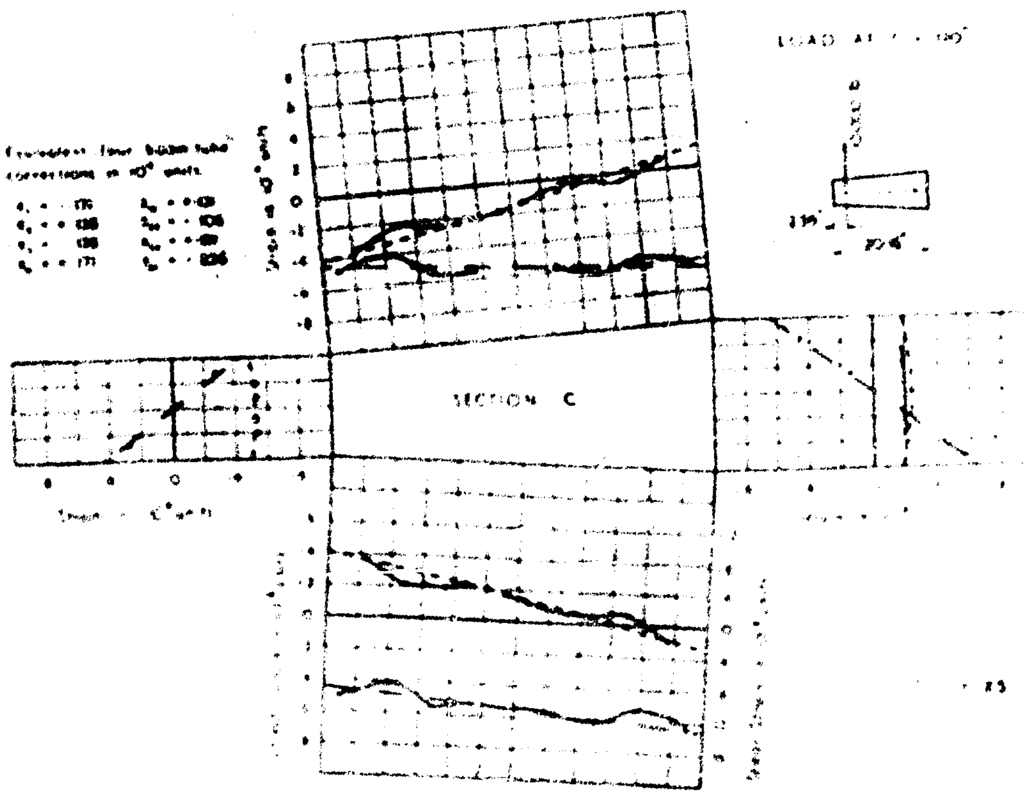

25

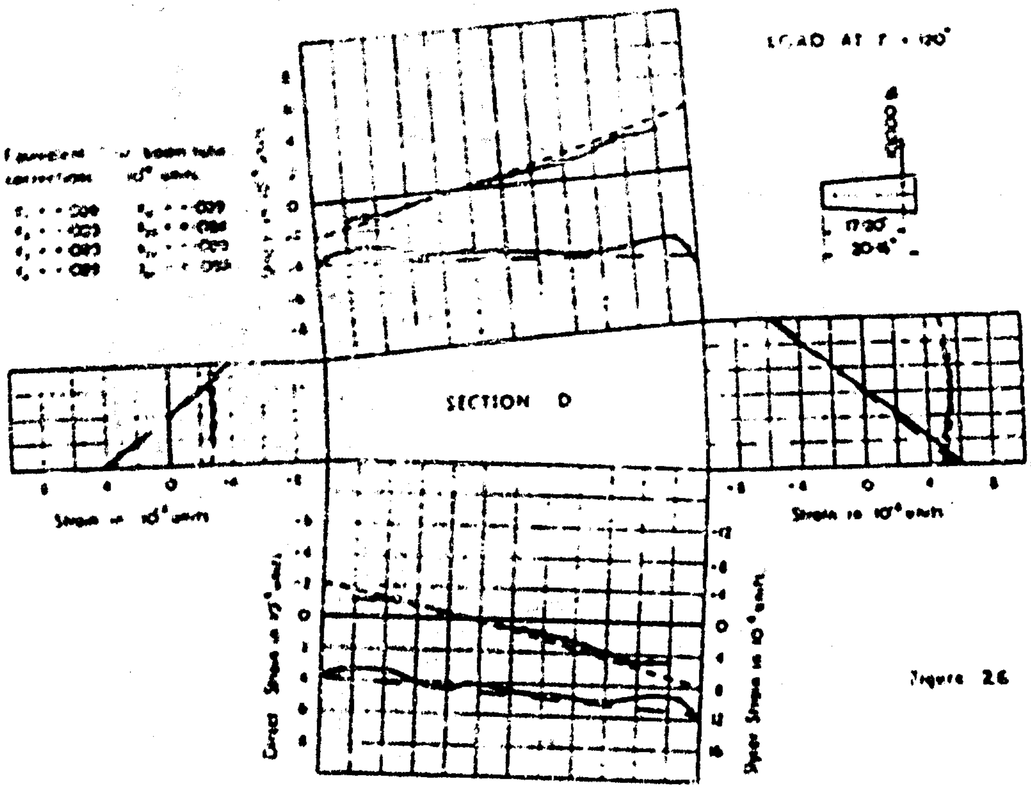

Figure 26

	Direct Strain	Shear Strain
Experiment	———	———
Elementary Theory	— — —	- - - - -

Tensile strains and anticlockwise shear strains are considered positive and are plotted outwards. The direct strains are drawn full scale and the shear strains half scale

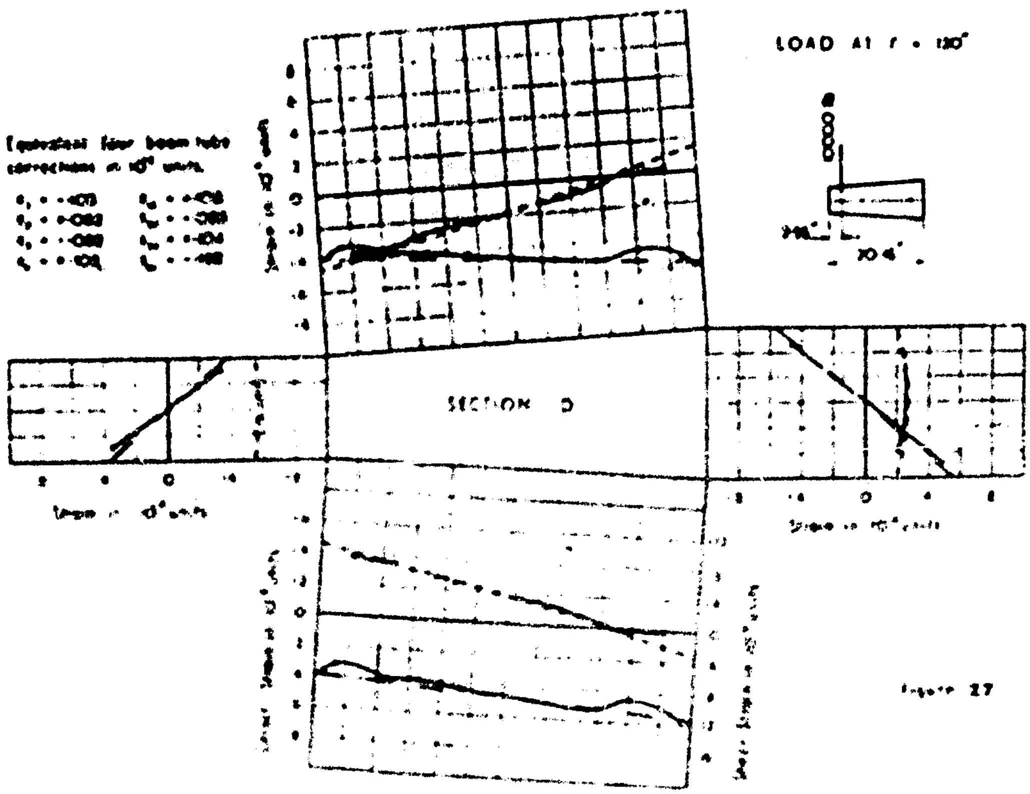

Figure 27

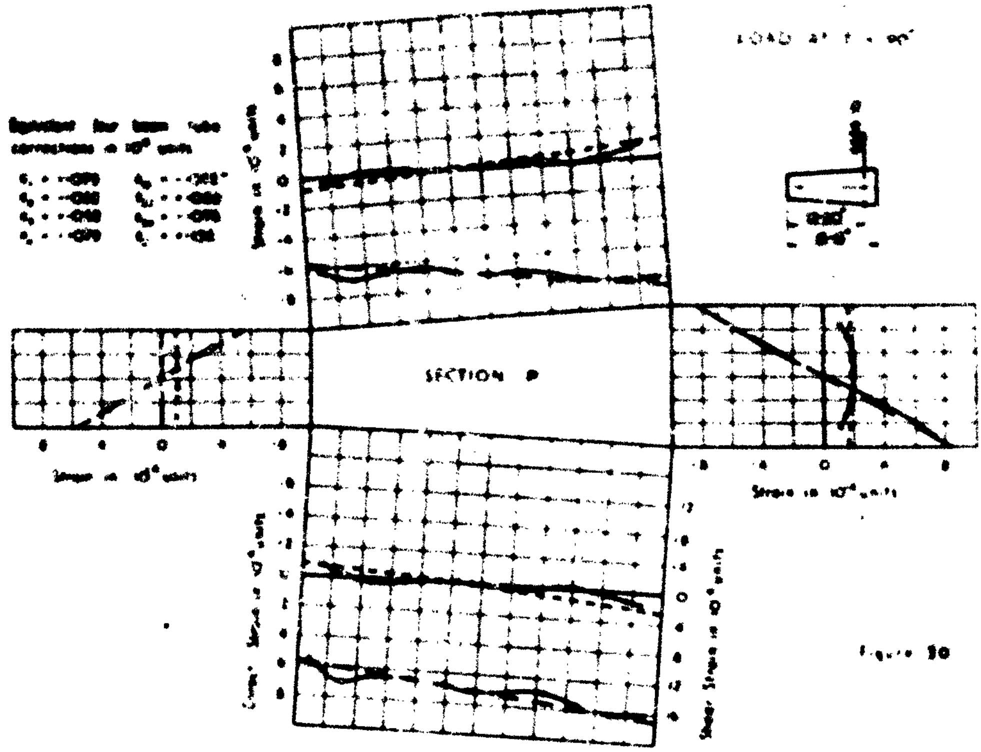

Figure 30

	Direct Strain	Shear Strain
Experiment	————	————
Elementary Theory	— — —	- - - - - -

Tensile strains and anticlockwise shear strains are considered positive and are plotted outwards. The direct strains are drawn full scale and the shear strains half scale.

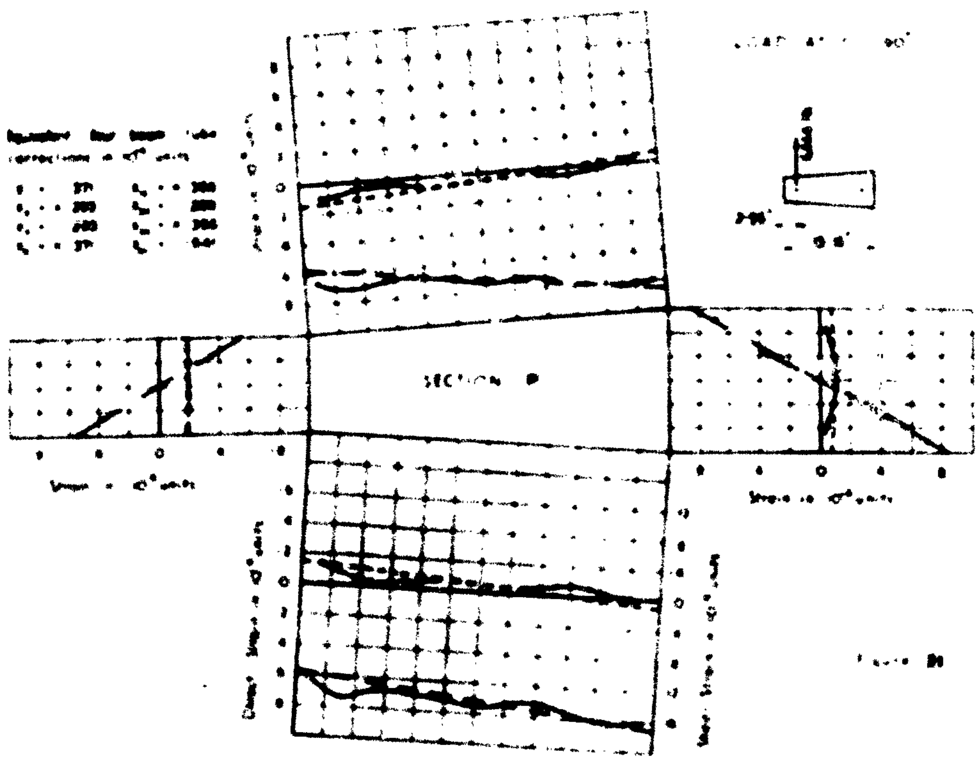

Figure 31

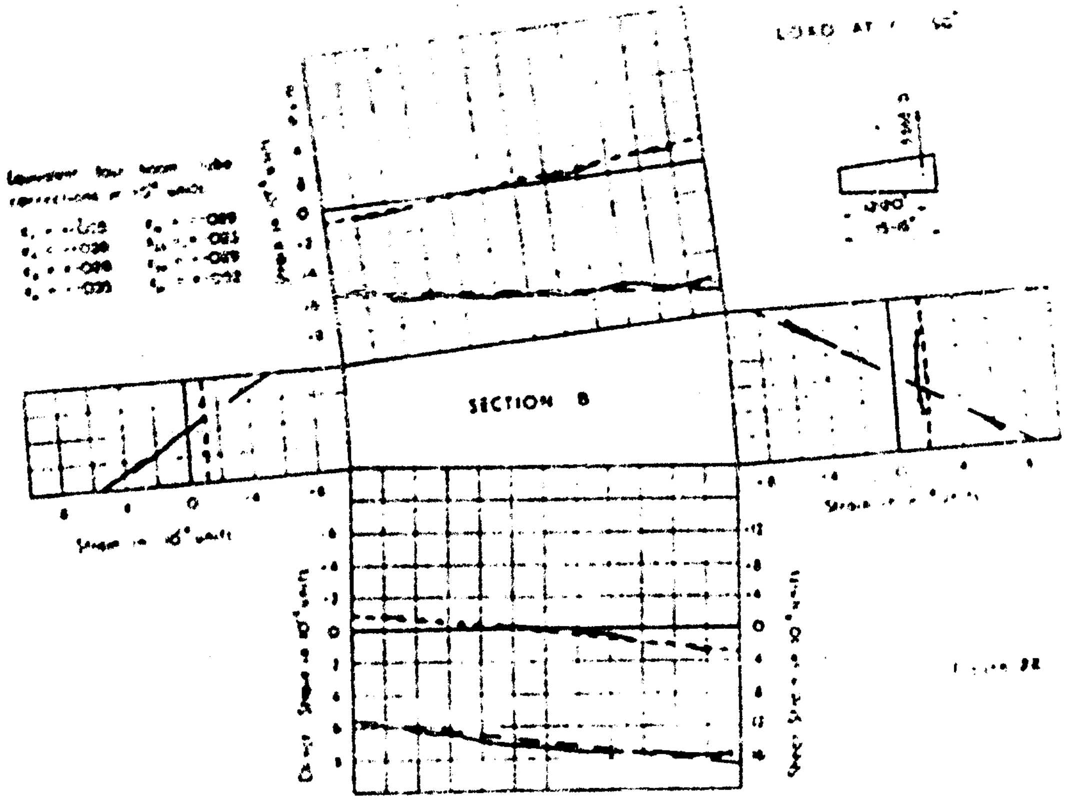

Figure 38

	Direct Strain	Shear Strain
Experiment	———	———
Elementary Theory	— — —	- - - - - -

Tensile strains and anticlockwise shear strains are considered positive and are plotted outwards. The direct strains are drawn to scale and the shear strains half scale.

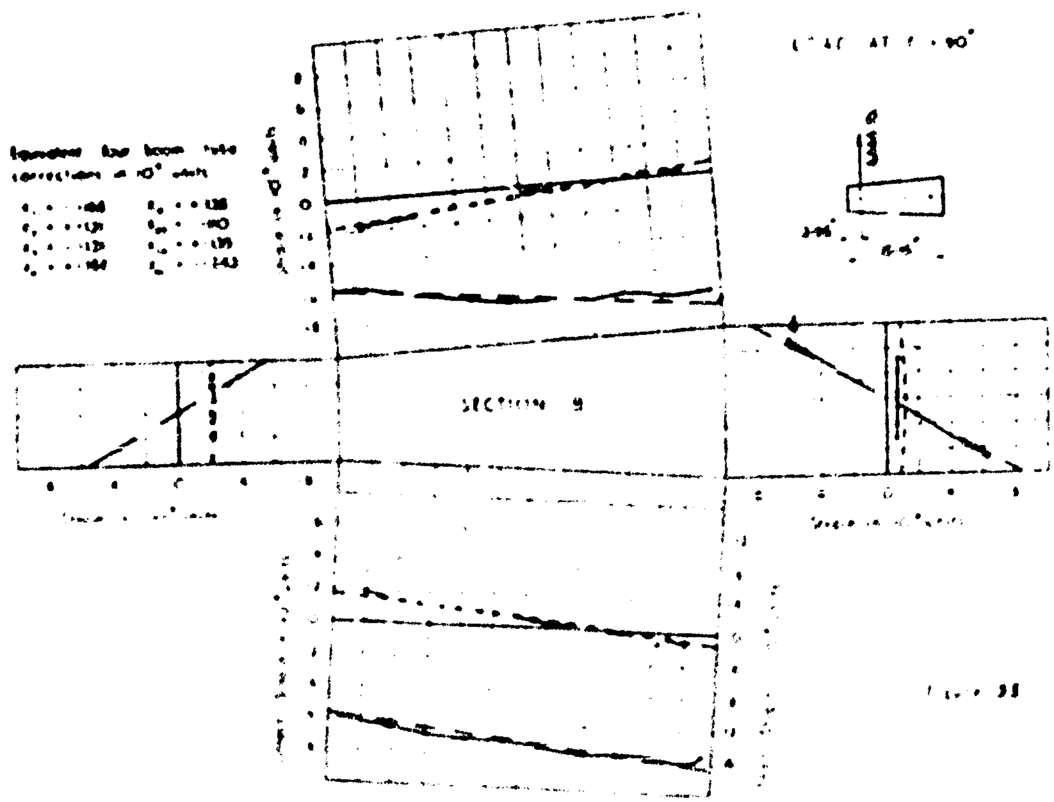

Figure 39

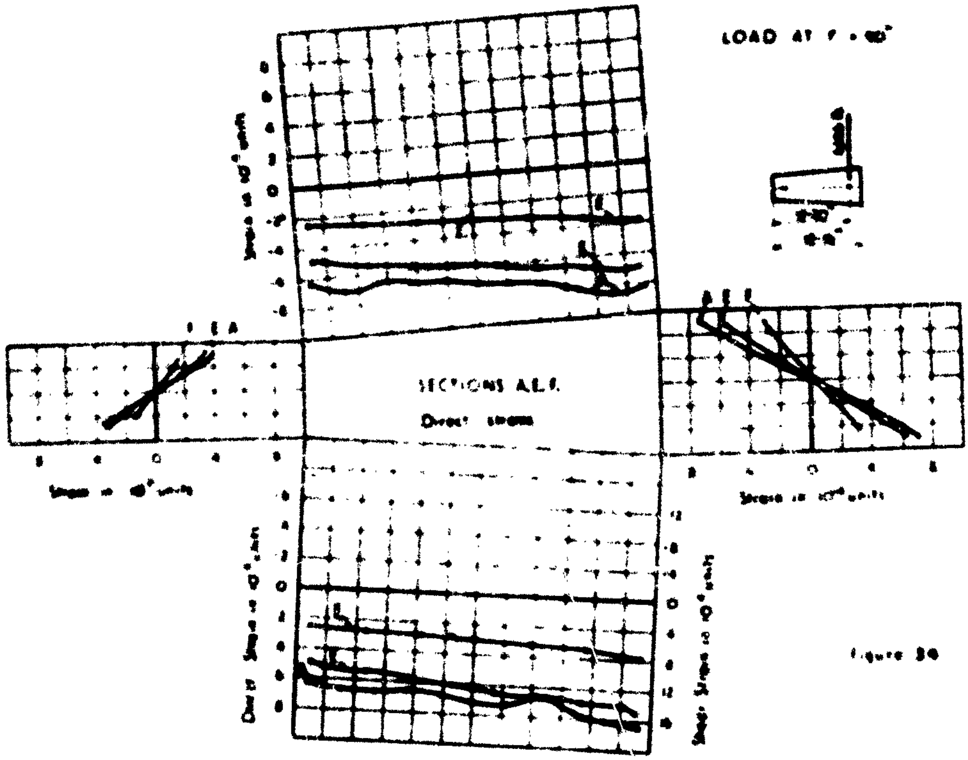

Figure 34

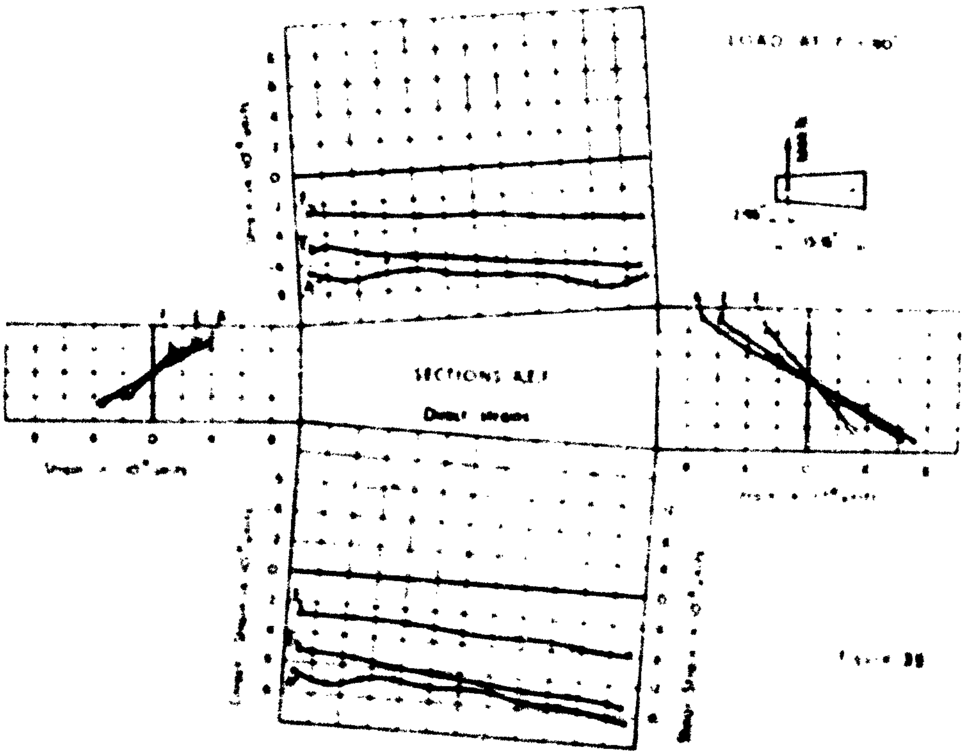

Figure 35

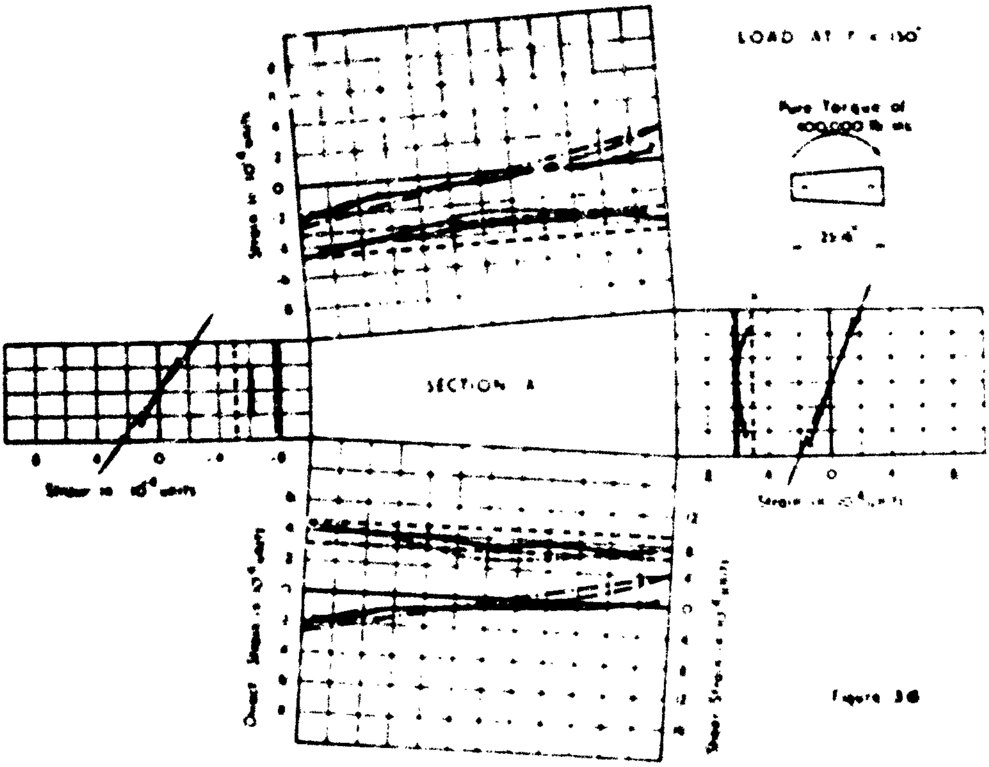

Figure 36

	Direct Strain	Shear Strain
Experiment	———	———
Elementary Theory	— — —	- - - - - -
Equivalent four boom tube	—·—·—	- - - - - -
Covers carrying direct stress	—·—·—	- - - - - -

Tensile strains and anticlockwise shear strains are considered positive and are plotted outwards. The direct strains are drawn full scale and the shear strains half scale.

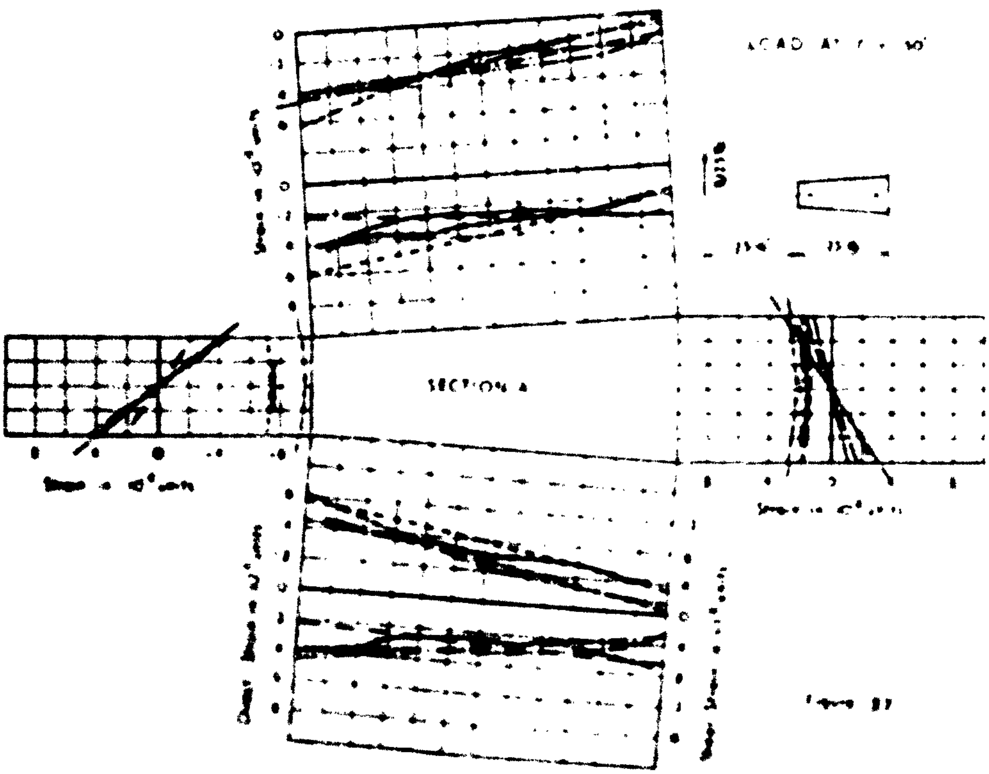

Figure 37

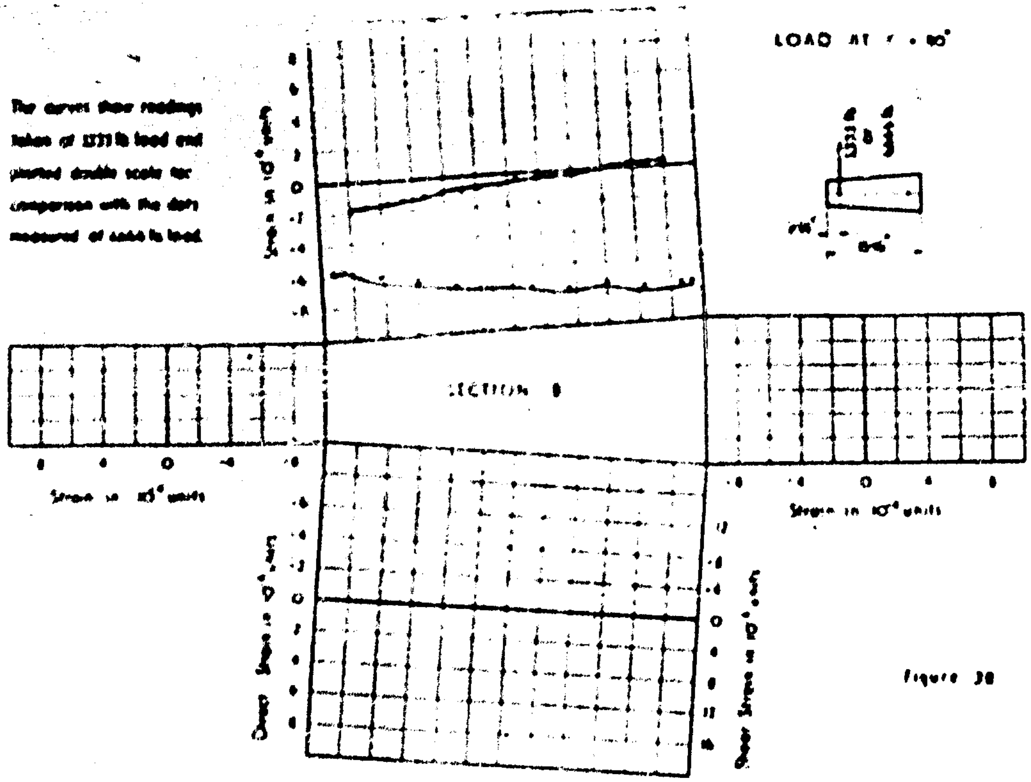

Figure 38

	Direct Strain	Shear Strain
Experiment	————	———•—•
Elementary Theory	— — —	- - - - - -
Equivalent four boom tube	—·—·—	-·-·-·- -
Covers carrying direct stress	——·——·	-·-·- -·-

Tensile strains and anticlockwise shear strains are considered positive and are plotted outwards. The direct strains are drawn full scale and the shear strains half scale.

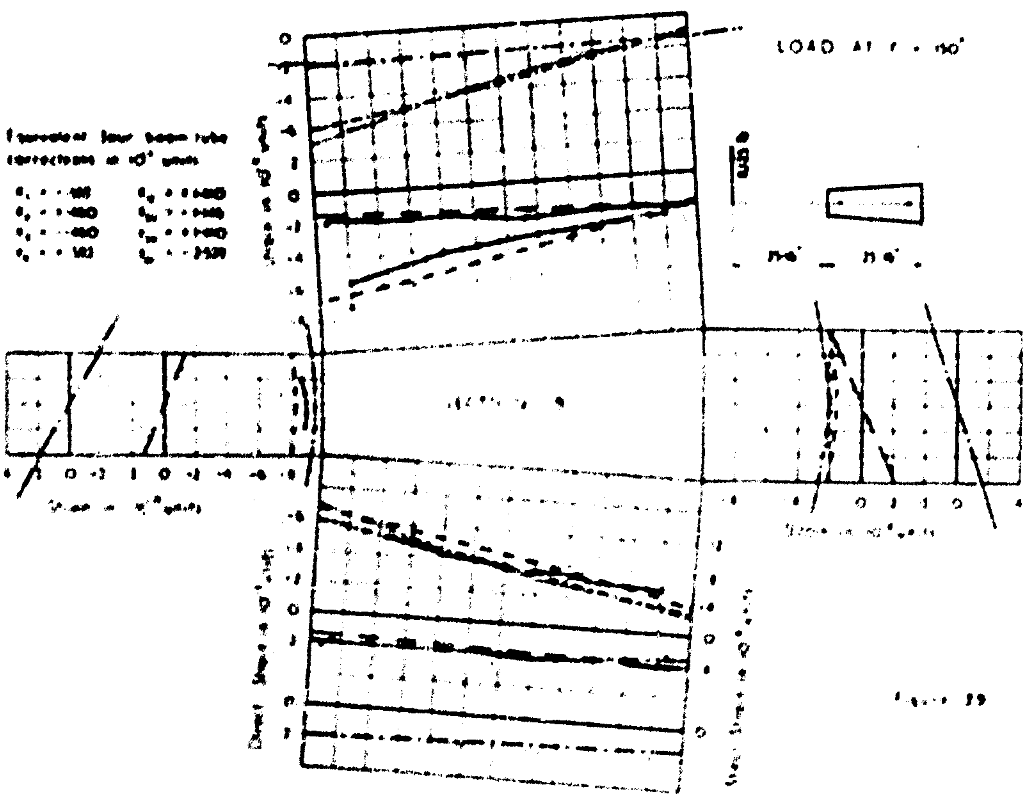

Figure 39

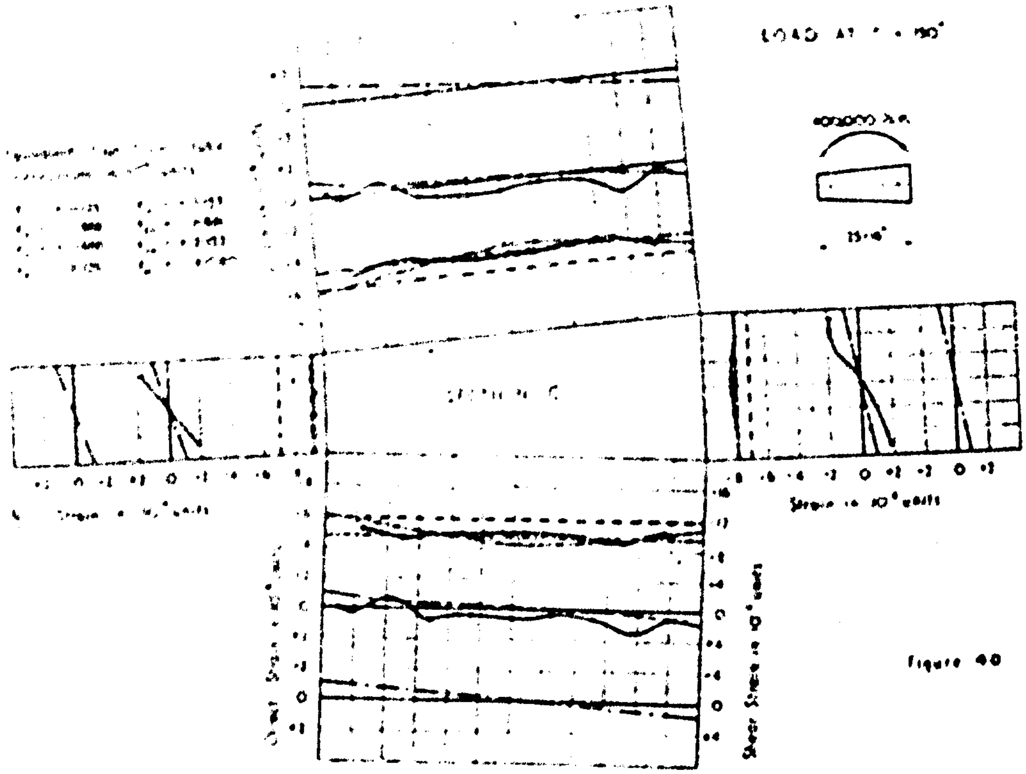

Figure 40

	Direct Strain	Shear Strain
Experiment		
Elementary Theory		
Equivalent four boom tube		
Covers carrying direct stress		

Tensile strains and anticlockwise shear strains are considered positive and are plotted outwards. The direct strains are drawn full scale and the shear strains half scale.

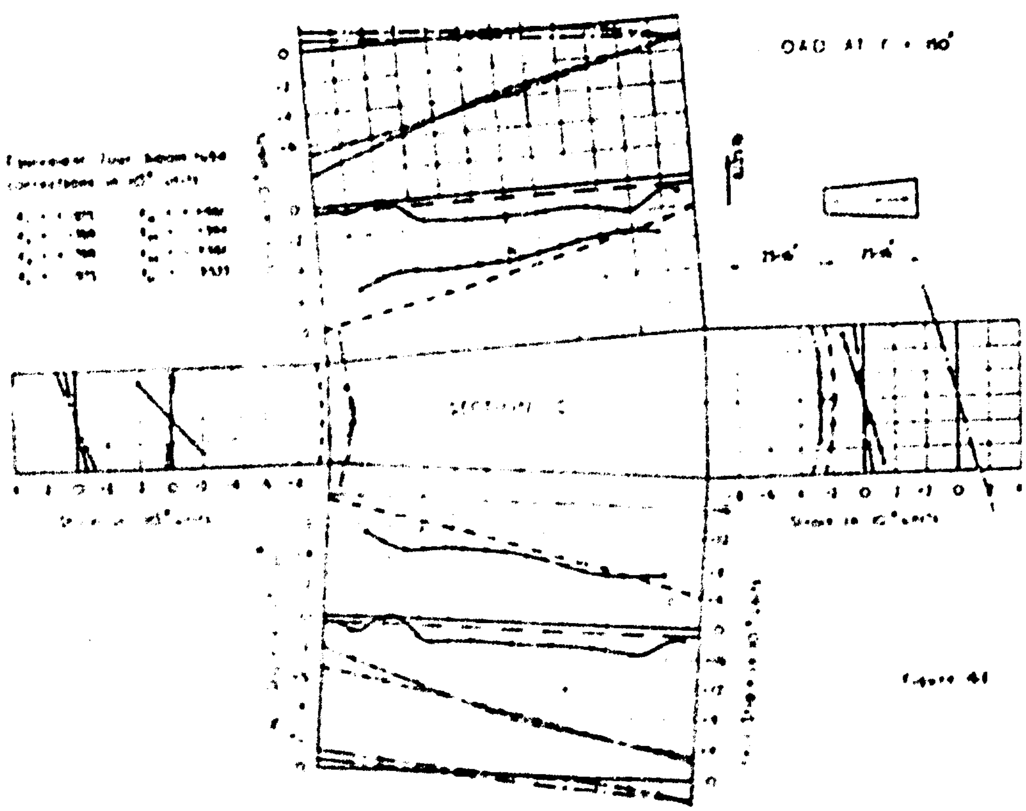

Figure 41

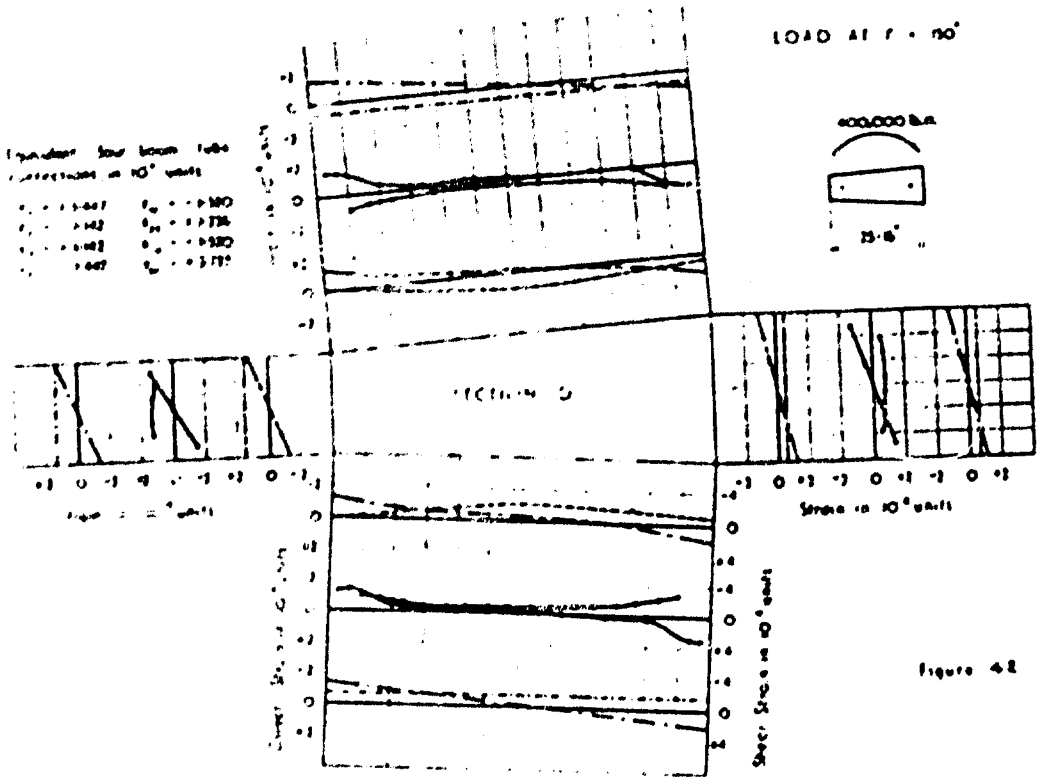

Figure 42

	Direct Strain	Shear Strain
Experiment		
Elementary Theory		
Equivalent four boom tube		
Covers carrying direct stress		

Tensile strains and anticlockwise shear strains are considered positive and are plotted outwards. The direct strains are drawn full scale and the shear strains half scale.

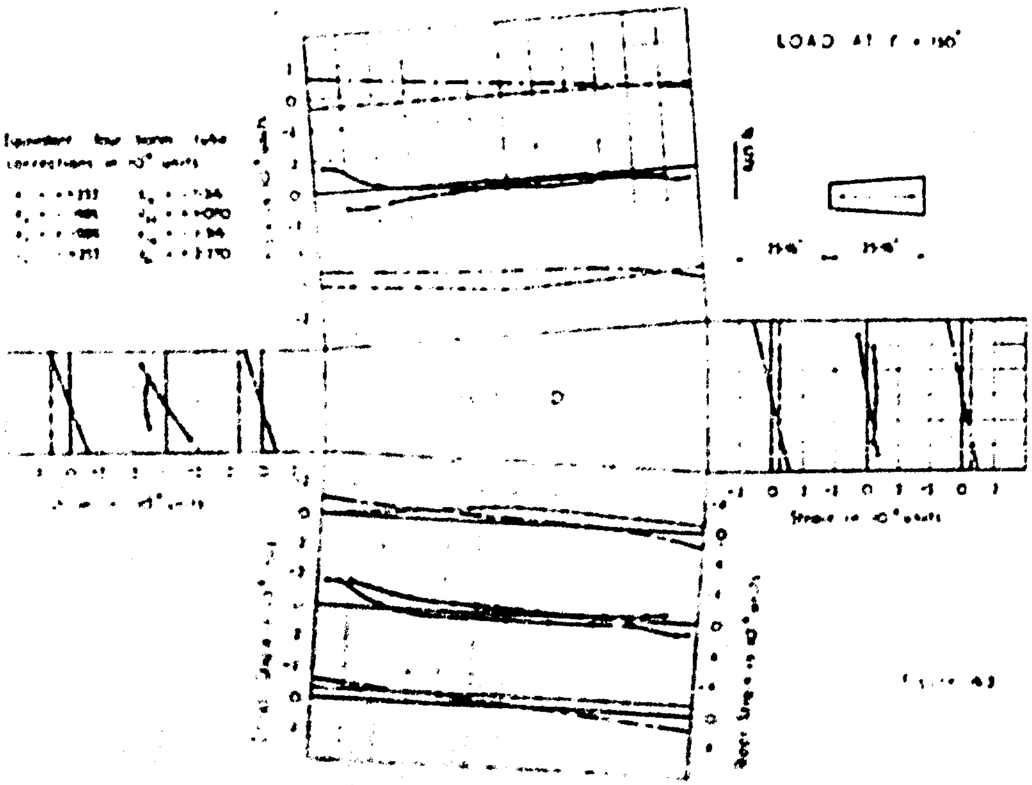

Figure 43

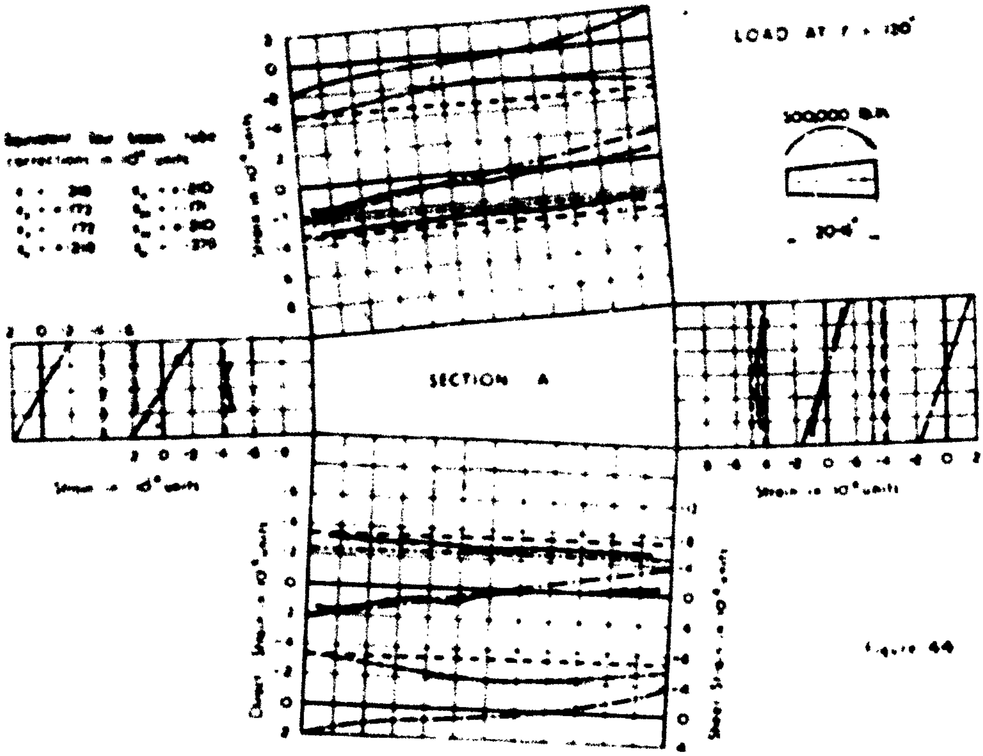

Figure 44

	Direct Strain	Shear Strain
Experiment		
Elementary Theory		
Equivalent four boom tube		
Covers carrying direct stress		

Tensile strains and anti-clockwise shear strains are considered positive and are plotted outwards. The direct strains are drawn full and the shear strains half.

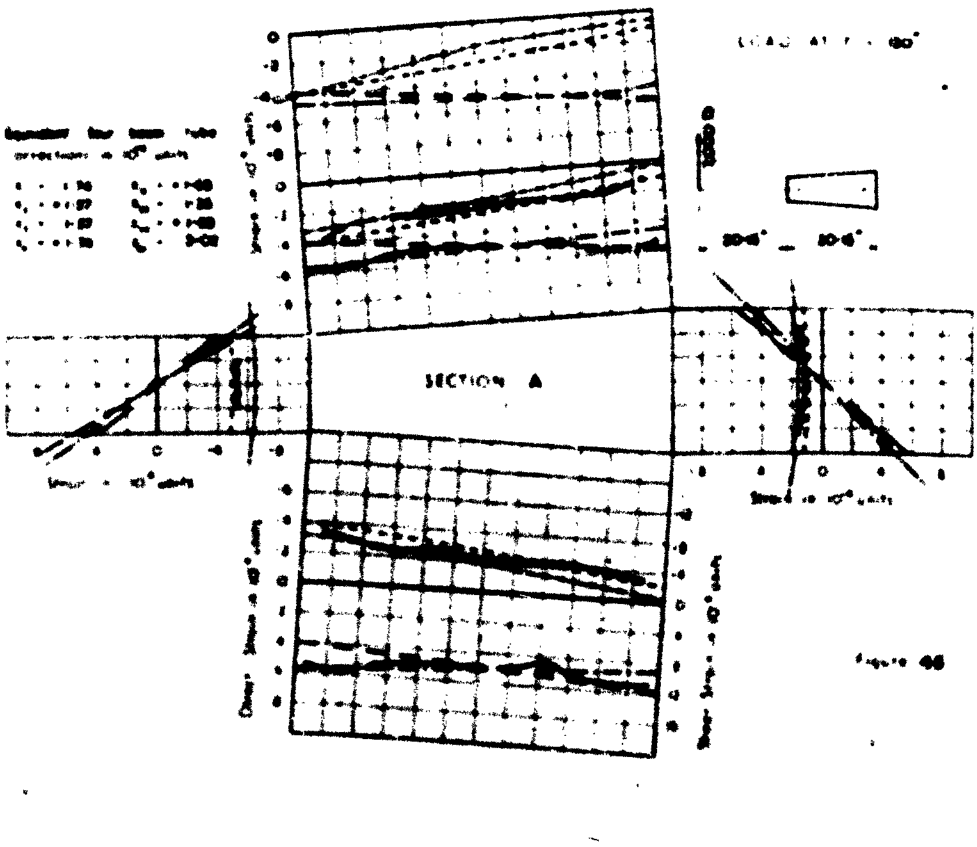

Figure 45

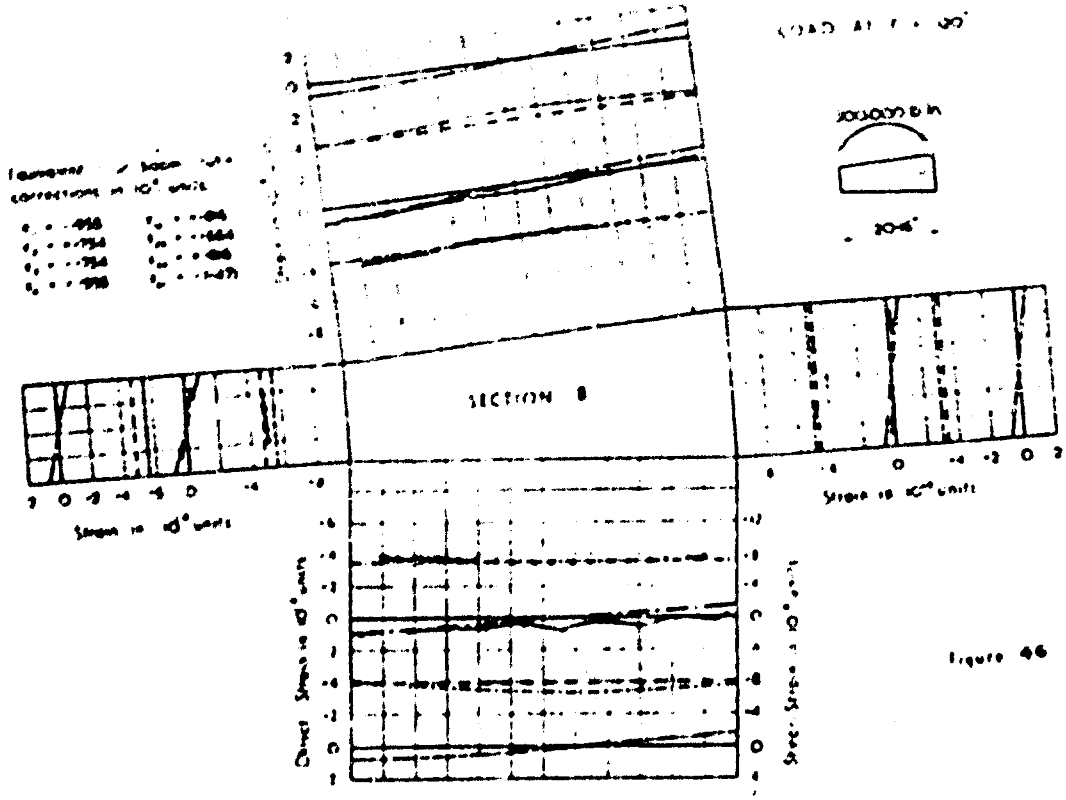

Figure 46

Direct Strain — Shear Strain

Experiment

Elementary Theory

Equivalent four boom tube

Covers carrying direct stress

Tensile strains and anticlockwise shear strains are considered positive and are plotted outwards. The direct strains are drawn full scale and the shear strains half scale.

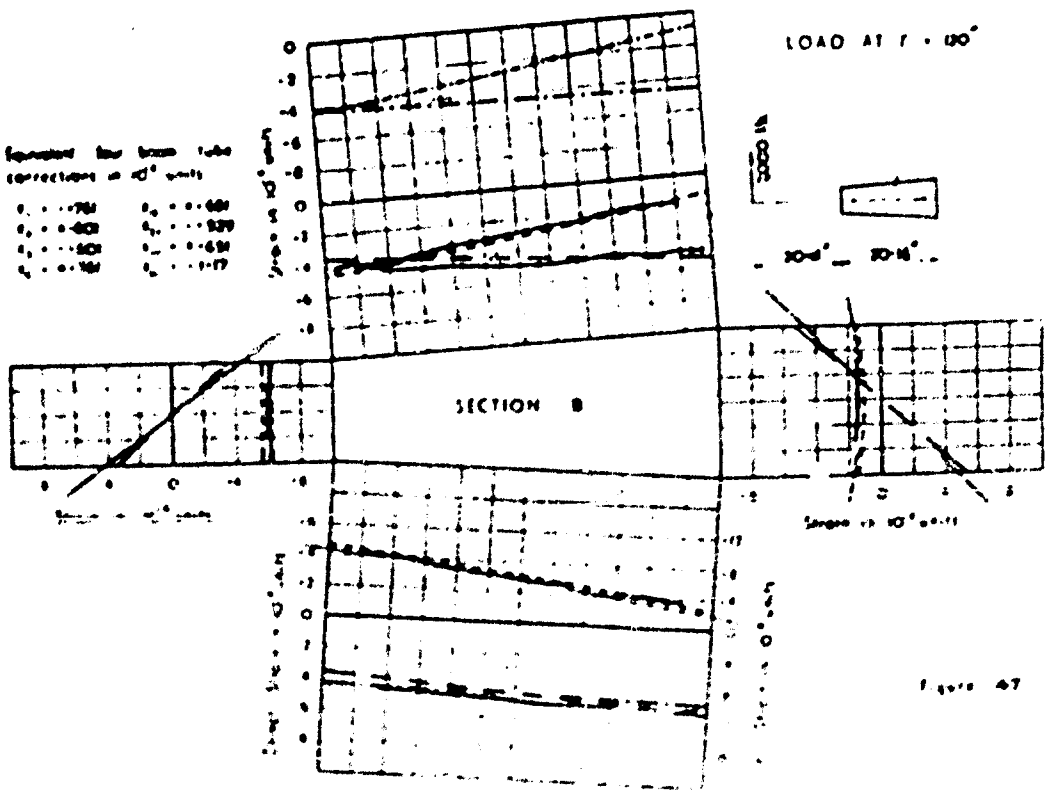

Figure 47

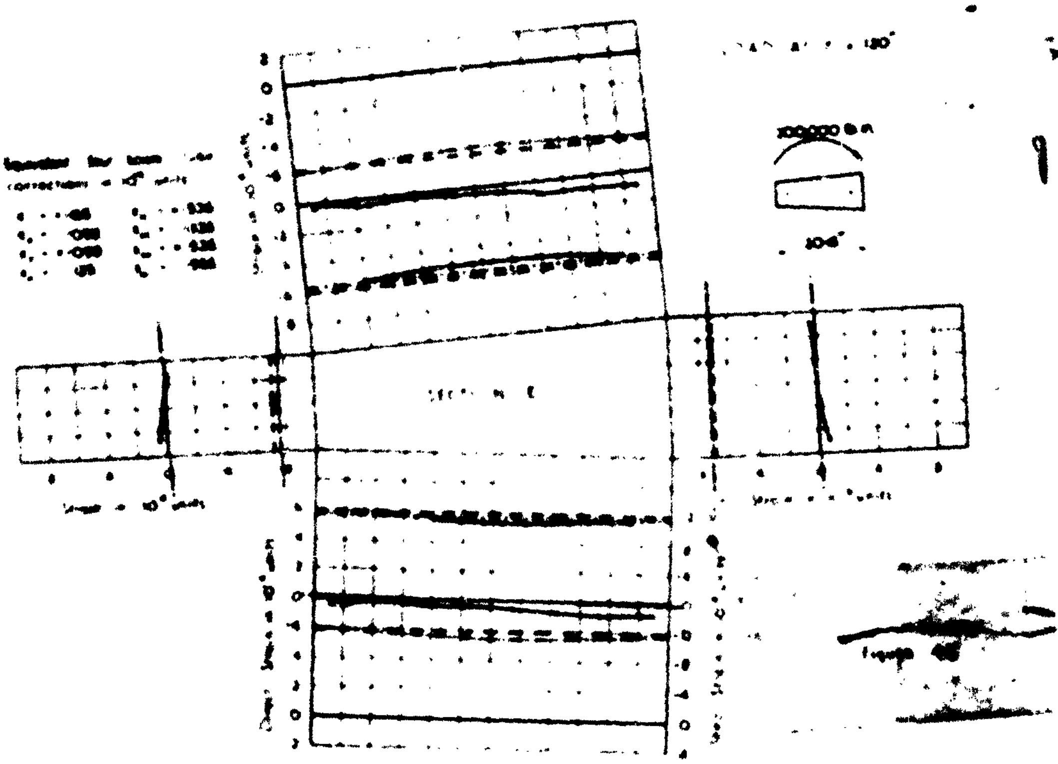

Figure 48

	Direct Strain	Shear Strain
Experiment		
Elementary theory		
Equivalent four boom tube		
Covers carrying direct stress		

Tensile strains and anticlockwise shear strains are considered positive and are plotted outwards. The direct strains are drawn full scale and the shear strains half scale.

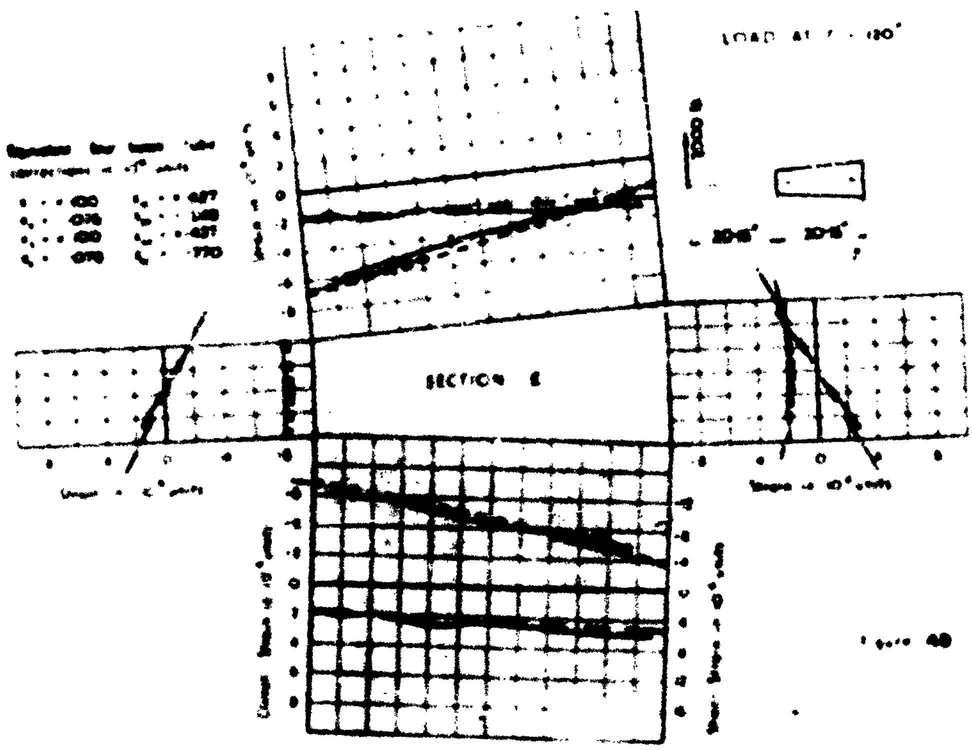

Figure 48

These curves were obtained by superimposing results for each load acting separately.

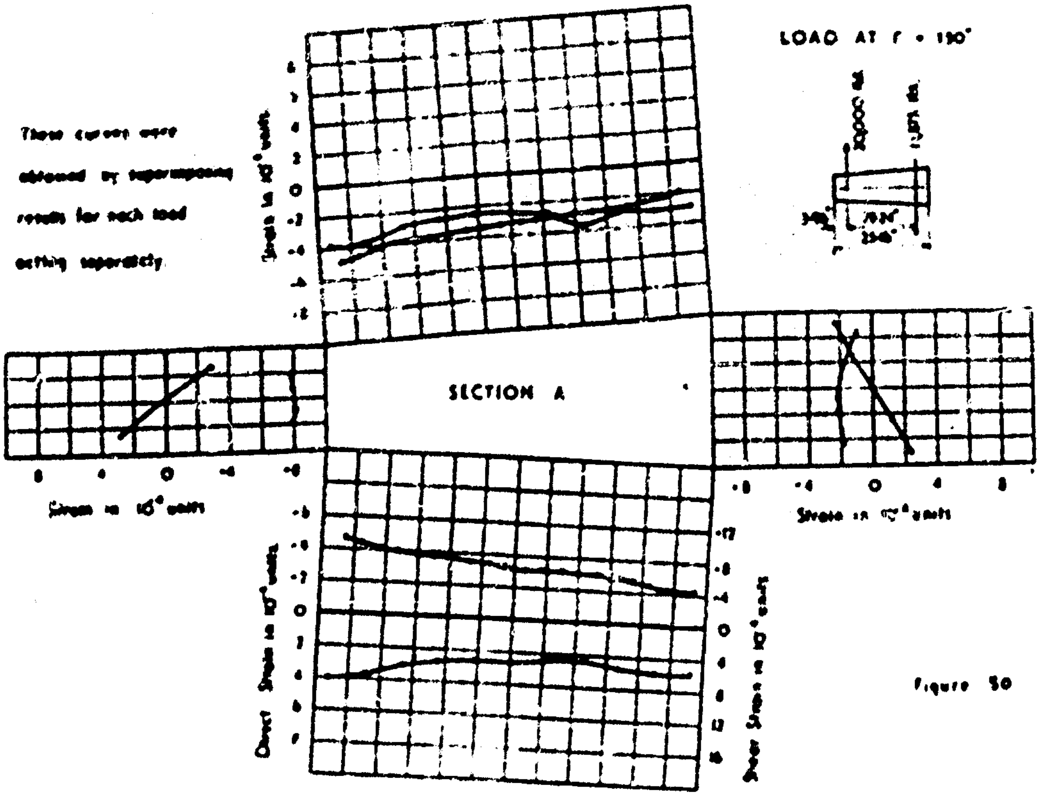

Figure 50

	Direct Strain	Shear Strain
Experiment		
Elementary Theory		
Equivalent Spar-beam Tube		
Covers carrying direct stress		

Tensile strains and anticlockwise shear strains are considered positive and are plotted outwards. The direct strains are drawn to scale and the shear strains half scale.

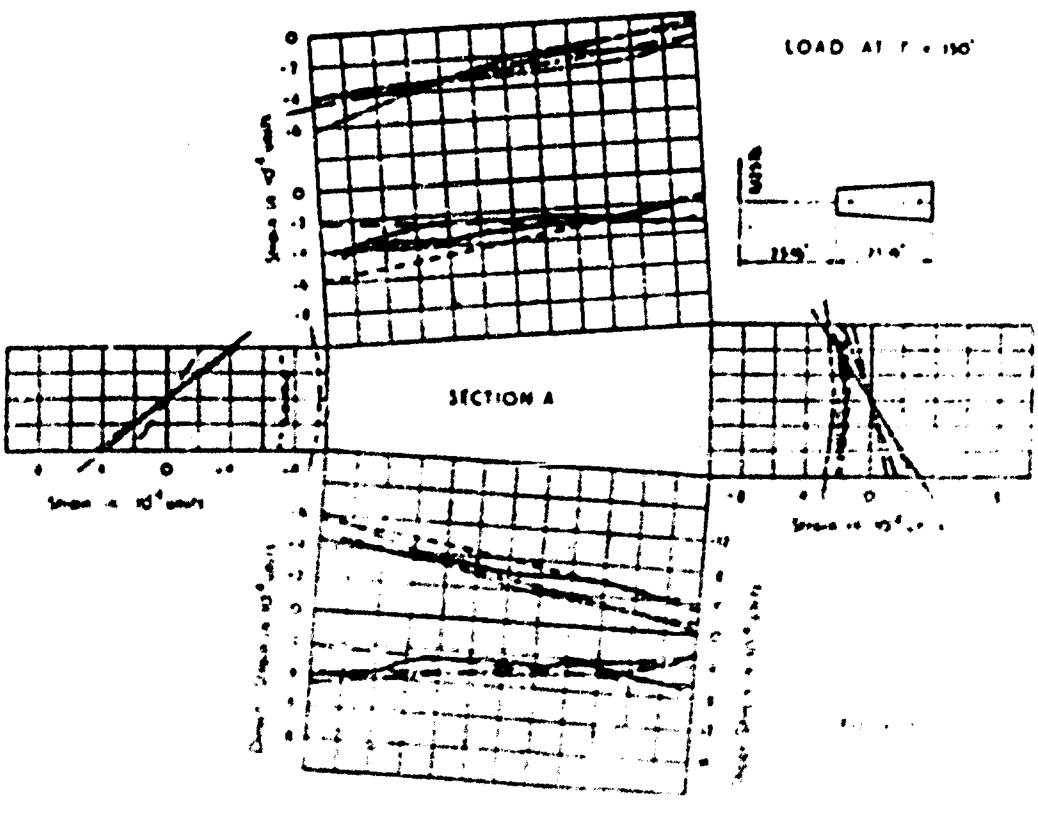

[illegible]

Table 7.

[illegible]

Table

[illegible]

Table 4.

[illegible]

Table 5.

[illegible]

Table

[illegible]

Table 3.

APPENDIX I

Brief Review of the Argyris and Dunne Theory

For convenience in presentation and use, Argyris and Dunne have given the results of their theory as correction stresses to be superimposed on stresses found by the conventional engineers' theories of bending and torsion. As stress distributions of the conventional theories are statically equivalent to the true stress distributions, the corrections have no statical resultants and have been called 'self balancing' or 'self equilibrating' stresses.

The authors have developed their theory from the conditions for elastic equilibrium of an infinitesimally small element of material. The following simplifying assumptions have been made.

1. If all generators were produced they would meet in a common point outside the tube.

2. The direct stress and strain normal to the generators are zero.

3. The shape of cross section of the tube is maintained by an indefinitely closely spaced system of diaphragms rigid in their own planes but offering no resistance to deflections out of their planes.

4. The diaphragms are all parallel to the root cross section.

5. The angle between any generator and an axis perpendicular to the diaphragms is so small that its square is negligible compared to unity and its cosine may be written as unity.

6. At any point the shear stress along a generator is assumed to have the same value as the shear stress parallel and normal to a diaphragm.

7. The shear modulus is associated with the shear strain parallel to the direction in which the sheet is forced by the diaphragms to be effectively rigid. The direct modulus is associated with the direct strain along generators.

The fundamental assumption of the theory is that the cross sectional shape of a tube is kept constant. From this it follows that the movement under load of any point on the tube can be defined by an axial warping displacement and by the body rotation and displacements of the cross section shape containing the point within its original plane. The three displacements and the rotation appear as variables in the analysis and the strains are written algebraically in terms of their derivatives. As any transverse direct stress in the walls of a tube is assumed to be zero only one equilibrium equation for the stresses at a point has to be satisfied. The major part of the analysis is concerned, in effect, with the solution or approximate solution of this equilibrium equation.

The existence of some stress function, F, for the tube is assumed which has the form of a function, g, of the distance from the taper point times a function, h, of the distance around the perimeter of the root cross section. By expressing the equilibrium equation in terms of the unknown stress function it has been possible to split it into two separate differential equations, one in terms of the geometry of the root cross section and the other in terms of the distance from the taper point. These give the transverse and longitudinal variations in stress.

The/

The equation involving the distance from the taper point has second order derivatives and its solution is not very difficult when the skin thicknesses are either constant or vary in a convenient manner with distance from the taper point.

The equation involving the geometry of the root cross section is linear and differential and has a separate solution with two arbitrary constants for each wall in which the thickness and slope are continuous functions. By considering the compatibility of direct strains and shear flows at each discontinuity around a cross section, an equation can be formed for each of these arbitrary constants. Together with the three equations of statics for equilibrium of the forces in a plane there are $2n + 3$ linear simultaneous equations for a tube where n is the number of walls. These equations have non-zero solutions when the determinantal equation is zero. In general the determinantal equation is transcendental and has an infinite number of roots.

The direct stress carrying ability of the walls has been treated analytically for only one specific case - that of a singly symmetrical tube with continuous direct stress carrying covers. In this case formulae are given for the determinantal equation and for the h function in each wall.

For utility an idealized tube is considered consisting of a number of direct stress carrying rods along generators connected by sheet of a purely shear resisting material. For the idealized tube the equation involving the geometry of the root cross section is algebraic instead of differential and there is only one arbitrary constant for each wall. There are $n + 3$ simultaneous equations and the determinantal equation has a finite number, $n - 3$, of roots. For an idealized tube having more than 6 - 8 booms the computation involved would be heavy.

The secular equation for an idealized four boom tube has but one root and for this case the theory finds its simplest application. Theoretical results for this case have been presented in a form which is immediately convenient for computation.

In general an allowance for the direct stress carrying ability of the walls of a tube may be made by assigning some portion of their cross sectional areas to adjacent booms or stringers. For the case of a four boom tube a rational procedure for this has been suggested by Argyris and Dunne.

APPENDIX II

Theoretical Computations

The curves of theoretical strain shown superimposed on the graphs of experimental results were computed according to:

(a) the elementary engineers' theories of bending and torsion,

(b) the theory of Argyris and Dunne for the case of an equivalent four boom tube,

(c) the theory of Argyris and Dunne for the case of a singly symmetrical tube with direct stress carrying top and bottom covers.

A brief record of the results and procedure of computation is given in this Appendix so that the reader may follow the main arguments of the analyses. In the account of the procedure according to Argyris and Dunne he is referred to the appropriate sections and equations of their "General Theory of Cylindrical and Conical Tubes under Torsion and Bending Loads".

Elementary Theory

The curves for strains by the elementary theories have been obtained from the formula

$$\frac{\sigma}{E} = \frac{M\bar{y}}{\rho^2 I_o E} \, ,$$

$$\frac{\tau_s}{G} = \frac{\tau_o}{G} - \frac{S}{t\,I_o G}\int_o^s t\,\bar{y}\,ds \, ,$$

and

$$\frac{\tau_b}{G} = \frac{T}{2\rho^2 A_o t G} \, ,$$

where the notation is, see Figs. 3a and 3b.

r		distance from taper point
r_o		distance from root to taper point
ρ	=	r/r_o
A_o		cross sectional area of tube at root
I_o		moment of inertia of tube at root
s		distance around perimeter of section from an origin at the root cross section

t/

t	wall thickness
$\bar{y}$	value of y corresponding to s
E, G	direct, and shear, elasticity moduli of material
S	applied shear force
M	bending moment at a section
M/r	shear load resisted by direct stress along generators
$Q = (S - M/r)$	shear load resisted by shear stresses
T	torsional couple about shear centre
σ	longitudinal direct stress
τ_c	component of shear stress due to Q
τ_o	value of τ_c at $s = 0$ if Q passed through shear centre
τ_b	component of shear stress due to torque T.

The corner angles, shown in Fig. 3a were considered to be concentrated as booms shown in Fig. 3b. In view of the simplicity of the expressions and as the work was halved by the single symmetry of cross section, shear strains were calculated at as many points around the cross section as seemed desirable (about fifty) for smooth curves to be drawn.

Equivalent four boom tube

An approximation to the axial constraint stresses was made by the method suggested in Appendix A.2.2. of the published theory of Argyris and Dunne. In discussing it, the notation, figure numbers and equations refer to text of that theory.

The dimensions of cross section Julon are shown in Fig.3b of this report were substituted in equations (A20), (A21) and (A22) of the Appendix giving the following boom areas corresponding to Fig.29;

$$B_1 = B_4 = 2.3799 \; , \quad B_2 = B_3 = 2.0266 \; .$$

These areas and the dimensions of cross section were then substituted in equation (193) of Part A.3 giving

$$\lambda^2 = 0.0[illegible]983 \; ,$$

and with λ in (44)

$$\lambda = 0.06[illegible] \; .$$

From (231), (237) and (239) the (H) functions were found to be

$$(H_\sigma)_1 = +5.163 \qquad (H_\tau)_{12} = +2.115$$
$$(H_\sigma)_2 = -4.074 \qquad (H_\tau)_{23} = -1.720$$
$$(H_\sigma)_3 = +4.074 \qquad (H_\tau)_{34} = +2.115$$
$$(H_\sigma)_4 = -5.163 \qquad (H_\tau)_{41} = -3.810$$

From (86a), $v = \mu r_o = 14.6490$, The G functions of (137a) and (137b), obtained with the use of (135a) and (135b) for values of r_1 = 90, 120 and 150 at each strain-gauged cross section are

	$\rho_1 = 0.8333$		$\rho_1 = 0.6666$		$\rho_1 = 0.5000$	
ρ	G_σ	G_τ	G_σ	G_τ	G_σ	G_τ
0.9833	+0.7763	-0.8164	+0.5652	-0.7950	+0.8696	-0.7939
0.9167	+0.2005	-0.4611	+0.3791	-0.3084	+0.3840	-0.3008
0.8528	-0.3351	-0.6414	+0.1827	-0.1332	+0.2085	-0.1079
0.8139	-0.4306	+0.4306	+0.1107	-0.1064	+0.1638	-0.0235
0.7500	-0.1411	-0.1411	-0.0494	-0.1026	+0.1412	-0.0120
0.5000	-0.0045	+0.0046	-0.1677	+0.1714	+0.1776	-0.0114
	G'_σ	G'_τ	G'_σ	G'_τ		

The correction components of stress were computed from (236a) and (236b) and then superimposed graphically on the strains of the elementary theories.

<u>Covers carrying direct stress</u>

Correction stresses were also found by the method given in Part 5.8 for a singly symmetrical trapezoidal tube. In this case the direct stress in the covers is considered, but the spar webs are treated as purely shear carrying. To make an allowance for the direct stresses in the webs, the boom areas shown in Fig. 3d, of this report, have been obtained by adding 1/6 of each web area to the adjacent booms of Fig. 3b.

By substituting the dimensions shown in the Fig. 3d in equation (48b), D = 4,672,600 and equation (135) simplified to

$$(-11270.6\lambda^4 + 413.919\lambda^2 + 0.124063)\ \frac{\sin(\lambda a_{12})}{(\lambda a_{12})}$$

$$+ (111.266\lambda^2 - 1.12407)\cos(\lambda a_{12}) + 1 = 0$$

This

This equation is transcendental and the first seven roots are

$$\lambda = 0,\ 0.119328,\ 0.157646,\ 0.[illegible]54259,\ 0.339556$$

$$0.439595,\ 0.537[illegible].$$

Solutions for equations (488) to (493) were then computed for each of the six non-zero values of λ and substituted in equations (495), (496) and (496a) in order to find H_σ, H_τ, $(H_\tau)_{23}$ and $(H_\tau)_{41}$. The H functions are listed in Table 3 for the webs and for seven equally spaced points across a cover, the dimension s, shown in the table, is measured from the centre of the cover.

The G functions were calculated for each of the values of λ from (137a) and (137b) and are listed in Tables 4, 5 and 6 for each strain gauge cross section.

Correction stresses were calculated from equations (136a) and (136b), or (319a) and (319b). By taking the first six significant values of λ, the distribution of strain around the cross sections was given by twelve terms of a trigonometric series. Table 7, which has been included as a sample, shows the calculation for Section A of the test box when a torque and a shear load were applied separately at $x = 150$ ($\rho_1 = 0.8333$). It will be seen from the table that convergence is reasonable for pure torque but is inadequate for bending. Further results for loading at $x = 150$ are summarised in Table 8.

It had been hoped initially that the terms would have been sufficiently convergent to interpret the shear lag effect in bending. Additional terms could have been computed. However as the labour of computation and tabulation of corrections for the tube with direct stress carrying covers was approximately 800 man hours, it was decided, after an inspection of the theoretical and experimental shear lag effects, that it would be unprofitable to spend further time on this aspect of the problem prior to submitting the report.

[dstl]

Information Centre
Knowledge Services
[dstl] Porton Down,
Salisbury
Wilts
SP4 0JQ
22060-6218
Tel: 01980-613753
Fax 01980-613970

Defense Technical Information Center (DTIC)
8725 John J. Kingman Road, Suit 0944
Fort Belvoir, VA 22060-6218
U.S.A.

AD#: AD011549

Date of Search: 30 May 2008

Record Summary: DSIR 23/20965
Title: Transversely Stiffened Tapered Box Girder under Torsion and Bending
Availability Open Document, Open Description, Normal Closure before FOI Act: 30 years
Former reference (Department) ARC 15128
Held by The National Archives, Kew

This document is now available at the National Archives, Kew, Surrey, United Kingdom.

DTIC has checked the National Archives Catalogue website (http://www.nationalarchives.gov.uk) and found the document is available and releasable to the public.

Access to UK public records is governed by statute, namely the Public Records Act, 1958, and the Public Records Act, 1967.
The document has been released under the 30 year rule.
(The vast majority of records selected for permanent preservation are made available to the public when they are 30 years old. This is commonly referred to as the 30 year rule and was established by the Public Records Act of 1967).

This document may be treated as UNLIMITED.